Am J Physiol Cell Physiol 298: C450–C456, 2010.
First published November 18, 2009; doi:10.1152/ajpcell.00077.2009.

Caveolin gene transfer improves glucose metabolism in diabetic mice

Koji Otsu,[1] Yoshiyuki Toya,[2] Jin Oshikawa,[2] Reiko Kurotani,[1] Takuya Yazawa,[3] Motohiko Sato,[1] Utako Yokoyama,[1] Satoshi Umemura,[2] Susumu Minamisawa,[1,4] Satoshi Okumura,[1] and Yoshihiro Ishikawa[1,5]

[1]Cardiovascular Research Institute, [2]Department of Cardiorenal Medicine, and [3]Department of Pathobiology, Yokohama City University Graduate School of Medicine, Yokohama, Japan; [4]Consolidated Research Institute for Advanced Science and Medical Care, Waseda University, Tokyo, Japan; and [5]Cardiovascular Research Institute, Departments of Cell Biology and Molecular Medicine and Medicine (Cardiology), New Jersey Medical School, Newark, New Jersey

Submitted 9 March 2009; accepted in final form 4 November 2009

Otsu K, Toya Y, Oshikawa J, Kurotani R, Yazawa T, Sato M, Yokoyama U, Umemura S, Minamisawa S, Okumura S, Ishikawa Y. Caveolin gene transfer improves glucose metabolism in diabetic mice. *Am J Physiol Cell Physiol* 298: C450–C456, 2010. First published November 18, 2009; doi:10.1152/ajpcell.00077.2009.— Caveolin, a member of the membrane-anchoring protein family, accumulates various growth receptors in caveolae and inhibits their function. Upregulation of caveolin attenuates cellular proliferation and growth. However, the role of caveolin in regulating insulin signals remains controversial. Here, we demonstrate that caveolin potently enhances insulin receptor (IR) signaling when overexpressed in the liver in vivo. Adenovirus-mediated gene transfer was used to overexpress caveolin specifically in the liver of diabetic obese mice, which were generated with a high-fat diet. Expression of molecules involved in IR signaling, such as IR or Akt, remained unchanged after gene transfer. However, hepatic glycogen synthesis was markedly increased with a decrease in phosphoenolpyruvate carboxykinase protein expression. Insulin sensitivity was increased after caveolin gene transfer as determined by decreased blood glucose levels in response to insulin injection and fasting blood glucose levels. Glucose tolerant test performance was also improved. Similar improvements were obtained in *KKA^y* genetically diabetic mice. Adenovirus-mediated overexpression of caveolin-3 in hepatic cells also enhanced IR signaling, as shown by increased phosphorylation of IR in response to insulin stimulation and higher glycogen synthesis at baseline. These effects were attributed mostly to increased insulin receptor activity and caveolin-mediated, direct inhibition of protein tyrosine phosphatase 1B, which was increased in obese mouse livers. In conclusion, our results suggest that caveolin is an important regulator of glucose metabolism that can enhance insulin signals.

insulin receptor; diabetes mellitus

CAVEOLIN (CAV) IS COMPOSED of three subtypes (Cav1, Cav2, and Cav3), and it is a major protein component of caveolae, which are flask-shaped, cell membrane invaginations that are abundantly expressed in adipocytes, myocytes, and endothelial cells (5). Caveolae accumulate multiple receptors and kinases that are involved in cell growth and proliferation (11, 19). The net effect of these interactions is the suppression of cellular growth and proliferation signals (5). Accordingly, it is widely believed that Cav is a potent growth suppressor.

Despite numerous studies demonstrating an important role for Cav in regulating various growth signals, the role of Cav in regulating insulin receptor (IR) signals has remained rather controversial. Some studies have shown a positive association of Cav with IR signals (3, 22) while others have refuted these findings (10). Nevertheless, it has been proposed that Cav may not inhibit insulin signals, but may be required or even activate this signaling pathway (28). Mice with a disrupted Cav1 gene, which is most abundantly expressed in adipocytes, showed decreased IR protein expression and developed insulin resistance in fat tissues (7). Similarly, mice with disrupted Cav3, which is abundantly expressed in the muscles (9), developed insulin resistance in the skeletal muscles (22). Furthermore, a previous study used purified proteins to demonstrate that a small peptide derived from Cav stimulated IR kinase activity in vitro; interestingly, this stimulation was more potent with a peptide derived from Cav3 than Cav1 (30). These findings have suggested that Cav plays an important role in maintaining physiological insulin signals in the major target organs of insulin action, i.e., the liver and fat tissues.

In the present study, we have addressed the role of Cav in the liver. The liver is a major insulin target that expresses only a small amount of endogenous Cav, suggesting that the liver, unlike fat tissues and skeletal muscles, does not require high Cav levels, at least, under normal conditions. We have examined the effect of Cav3 gene transfer to the livers of diabetic obese mice fed a high-fat diet or *KKA^y* mice, a widely used Type 2 diabetic model (17). We demonstrated that Cav enhances IR signaling in vivo and in vitro. Insulin sensitivity and thus glucose metabolism were markedly improved by Cav3 gene transfer in diabetic mice, as exemplified by increased hepatic glycogen synthesis and improved glucose tolerance test performance.

MATERIALS AND METHODS

Diabetic mouse models. At weaning, mice (3 wk of age) were placed on either a high-fat diet (59% of calories derived from fat) for diabetic obese mice or a normal chow diet (10% of calories derived from fat) for lean normal mice (Oriental Yeast, Tokyo, Japan) for at least 6 mo. Differences in body weight became significant at 5 wk (Fig. 1*A*). At 6 mo, fasting blood glucose (FBG) levels were increased approximately threefold (Fig. 1*B*) and serum triglycerides by 20% (Fig. 1*C*) in obese diabetic mice relative to lean normal mice.

KKA^y mice were purchased from CLEA Japan (Tokyo, Japan) and used for experiments at 10 wk old. All animals were maintained in accordance with the guidelines of the animal experiment committees of Yokohama City University, and experiments were approved by the Ethical Committee of Animal Experiments of Yokohama City University School of Medicine.

Adenovirus construction and injection into mice. Full-length cDNA encoding rat Cav3 was cloned into the shuttle vector to construct an adenoviral vector harboring Cav3 or green fluorescent protein (GFP; control) using an AdenoX adenovirus construction kit (Clontech, Palo

Address for reprint requests and other correspondence: Y. Ishikawa, Cardiovascular Research Institute, Yokohama City University Graduate School of Medicine 3-9 Fukuura, Kanazawa-ku, Yokohama 236-0004, Japan.

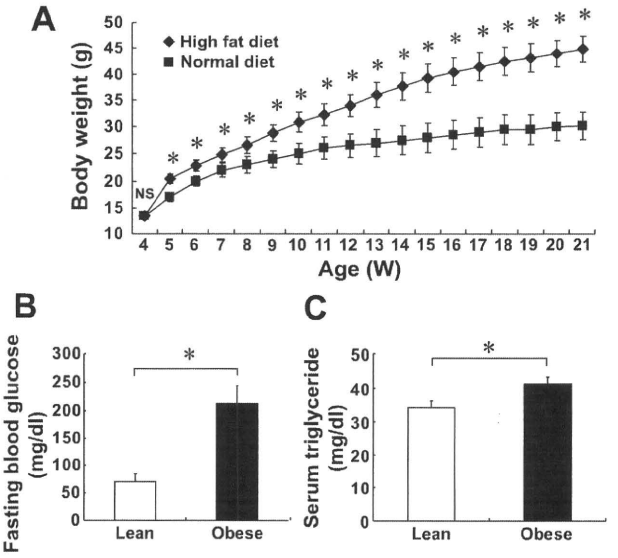

Fig. 1. Generation of obese diabetic mice. *A*: changes in body weight between obese mice and age (W, weeks)-matched, normal lean mice ($n = 31$, $^*P < 0.05$; NS, not significant). *B* and *C*: comparison of fasting blood glucose levels ($n = 8$–13, $^*P < 0.05$) (*B*) and serum triglycerides ($n = 4$–5, $^*P < 0.05$) (*C*) between lean control (Lean) and obese diabetic (Obese) mice.

Alto, CA) (11). An adenovirus titer of 1.0×10^7 plaque-forming units (PFU) was sufficient to overexpress Cav3 in the liver to levels equivalent to endogenous Cav3 in the skeletal muscles, where Cav3 is most abundantly expressed, for up to 6 days after viral injection (Fig. 2, *A* and *B*).

Radioligand binding assays and Western blot analysis. Radioligand binding assays for cell surface IR were performed using HepG2 cells and ^{125}I-labeled insulin as previously described (20, 24). Immunoblotting of Cav, IR-β, and its related molecules was performed as previously described (21, 22).

Immunoprecipitation assays. An in vivo phosphorylation assay for IR-β or insulin receptor substrate (IRS) was performed as previously described (22). After anesthesia was induced with pentobarbital sodium intraperitoneally (100 mg/kg ip), tissues were quickly harvested and stored in liquid nitrogen. Immunoprecipitation of Cav, IR-β, and its related molecules was performed as we previously described (22).

Protein fractionation by the sucrose gradient method. Caveolae fractions were separated by the sodium carbonate-based, detergent-free method (26, 30).

Glucose and insulin tolerance tests. After a 16-h period of fasting, glucose (2 mg/g body wt ip) was injected. FBG levels were determined at 0, 30, 60, 90, and 120 min after injection using a glucometer (22). For the insulin tolerance test, insulin was injected (0.75 U/kg ip), and then FBG levels were measured (7).

Measurements of hepatic glycogen synthesis and triglycerides. Glycogen was measured as previously described (27). Briefly, livers were homogenized in 6 M perchloric acid. The homogenate was boiled for 5 min at 100°C and centrifuged at 10,000 *g*. Glycogen in the supernatant was precipitated with ethanol and measured by a phenol-sulfuric acid reaction. Hepatic triglycerides were extracted as described previously (13). Briefly, tissues were homogenized in extraction buffer (20 mM Tris, pH 7.3, 1 mM EDTA, and 1 mM β-mercaptoethanol), after which chloroform, methanol, and water were added. The mixture was centrifuged at 3,000 *g*. The lower phase was evaporated and redissolved in isopropanol, and triglyceride concentrations were determined with the GPO-Trinder (Sigma, St. Louis, MO).

Measurements of serum lipids. Total cholesterol and triglycerides were determined as we described previously (22).

Cell culture. HepG2 cells, a human hepatocellular carcinoma cell line, were cultured in Dulbecco's modified Eagle's medium containing 5% fetal bovine serum and 10% horse serum in a humidified 95% air-5% CO_2 incubator.

Inhibition of phosphatase activity by Cav peptides. Phosphatase activity was measured colorimetrically using a commercial assay kit (Calbiochem, San Diego, CA) and purified protein tyrosine phosphatase 1B (PTP1B) (Upstate, Lake Placid, NY) in the presence or absence of the following Cav peptides; for the scaffolding domain

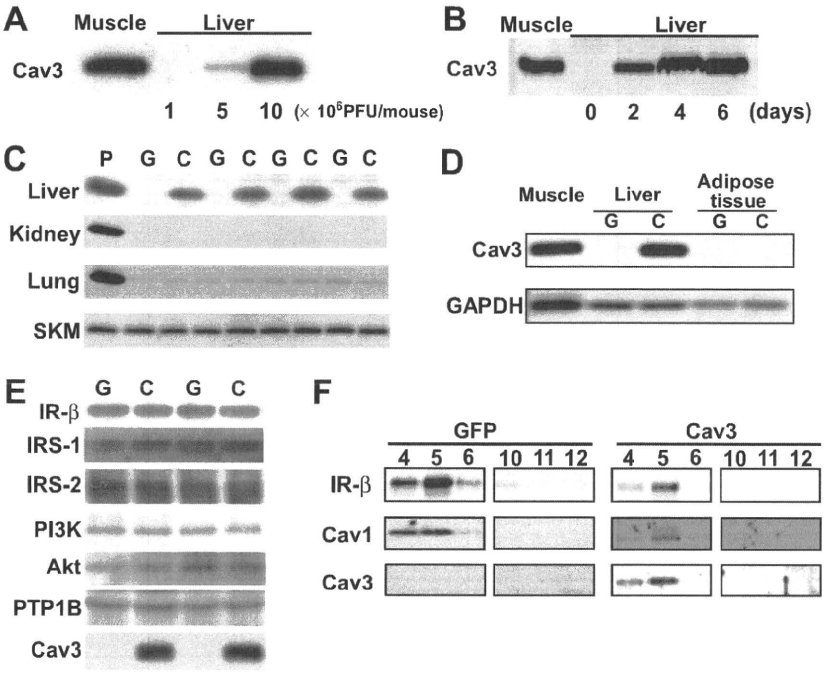

Fig. 2. Caveolin-3 (Cav3) gene transfer to the liver. Adenovirus harboring the Cav3 or green fluorescent protein (GFP) gene was injected into the tail veins of mice. *A*: dose-dependent Cav3 expression in whole liver homogenates. Adenovirus harboring the Cav3 or GFP (control) gene was injected at 0, 1, 5, or 10×10^6 plaque-forming units (PFU). An equivalent amount of total protein from muscle samples was used as positive control (*left lane*). *B*: time-dependent Cav3 expression in the liver. Livers were harvested at 2, 4, and 6 days after injection and analyzed by immunoblotting. *C*: Cav3 expression in various organs of mice after Cav3 gene transfer (C) vs. GFP gene transfer (G). Cav3 protein expression was detected only in the liver. Muscle was used as positive control (P). SKM, skeletal muscle. *D*: Cav3 expression after Cav3 gene transfer in adipose tissues. GAPDH is shown as loading standard. *E*: expression of molecules involved in insulin receptor (IR) signaling in hepatic tissues after Cav3 or GFP gene transfer. IRS-1 and 2, insulin receptor substrate 1 and 2; PTP1B, protein tyrosine phosphatase 1B; PI3K, phosphatidylinositol 3-kinase. *F*: sucrose gradient fractionation of liver proteins and immunoblotting of exogenous Cav3, endogenous Cav1, and IR-β (*lanes 4*, *5*, and *6*, caveolar fractions; *lanes 10*, *11*, and *12*, noncaveolar fractions)

(SD) peptide: Cav3 (SD-Cav3)-DGVWRVSYTTFTVSKYWCYR; Cav1 (SD-Cav1)-DGIWKASFTTFTVTKYWFYR; for the nonscaffolding domain (NSD) peptide: Cav3 (NSD-Cav3)-NRDPKNINEDIVKVDFEDVIAEPEG; Cav1 (NSD-Cav1)-NRDPKHLNDDVVKIDFEDVIAEPEG. Briefly, purified PTP1B (0.022 units) was incubated with increasing concentrations of Cav peptide (0, 0.63, 1.25, 2.5, 5, and 10 μM) at room temperature for 10 min, followed by the addition of the enzyme substrate and an additional 15-min incubation. PTP1B activity was determined by spectrophotometry.

RESULTS

Overexpression of Cav3 in the liver. The liver expressed relatively small amounts of endogenous Cav1, and little Cav3 was detected by immunoblotting mouse liver homogenates. Using the Cav3 adenovirus (1.0×10^7 PFU), Cav3 expression in liver homogenates was comparable to that of endogenous Cav3 in the skeletal muscle (Fig. 2*A*), another major organ involved in regulating glucose metabolism that abundantly expresses Cav. With this amount of adenovirus, the expression of Cav3 peaked at *day 4* postinjection and plateaued at least until *day 6* (Fig. 2*B*). The gene delivery of Cav3 was restricted to the liver, and there was no increase in Cav3 expression in the other organs such as skeletal muscles or adipose tissues (Fig. 2, *C* and *D*). Despite Cav3 overexpression, the protein expression of IR-β as well as other molecules involved in IR signaling such as IRS, phosphatidylinositol 3-kinase (PI3K), Akt, or PTP1B were unchanged (Fig. 2*E*), suggesting that Cav3 does not regulate the protein expression of these molecules, at least, in the liver. The subcellular distribution of exogenous Cav3 and endogenous IR-β, as determined by sucrose gradient fractionation of liver tissues, was unchanged and similar to that of endogenous Cav1 (Fig. 2*F*), and insulin binding assays using intact hepatic cells revealed no changes in B_{max} [GFP vs. Cav3: 4.2 ± 0.1 vs. 4.3 ± 0.2, $n = 4$, P = not significant (NS)] or K_d (GFP vs. Cav3: 58.4 ± 0.1 vs. 58.9 ± 0.4 fmol, $n = 4$, P = NS) with Cav3 gene transfer, suggesting that Cav3 gene transfer did not alter the caveolar and/or the cell surface localization of IR.

Cav3 gene transfer is associated with increased glycogen synthesis in the liver. Because one of the most important actions of insulin is to promote glycogen synthesis in tissues (23), we examined whether Cav3 gene transfer changed the glycogen content in the livers of diabetic obese mice and found that it was significantly increased in mice with Cav3 gene transfer (Fig. 3*A*). Fat deposition was similar in the livers of diabetic obese mice with Cav3 gene transfer and GFP gene transfer, indicating that it was caused by a high-fat diet and not by Cav3 overexpression. The increase in glycogen content in mice with Cav3 gene transfer was accompanied by a decrease in protein expression of the cytosolic form of phosphoenolpyruvate carboxykinase (PEPCK) (Fig. 3*C*). This enzyme catalyzes the first irreversible reaction in gluconeogenesis, and the activity of PEPCK is proportional to the amount of this

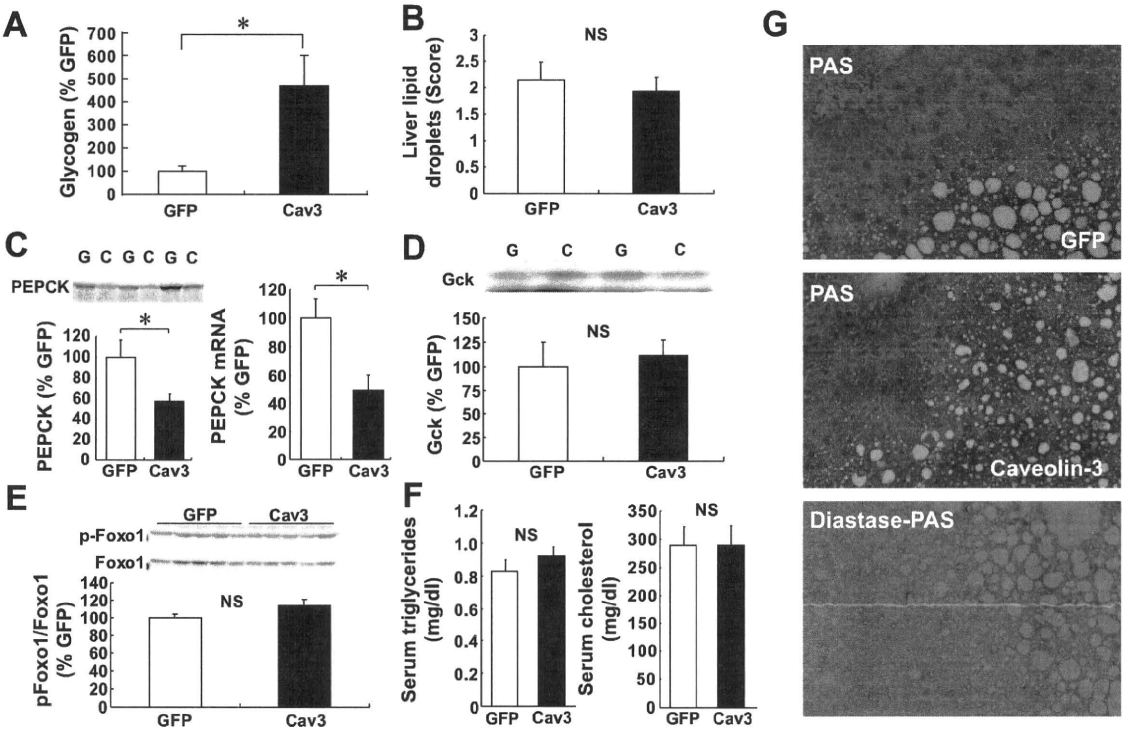

Fig. 3. Increased glycogen content in the liver after Cav gene transfer. *A*: hepatic glycogen content at baseline after Cav3 vs. GFP gene transfer in diabetic obese mice ($n = 4$, $^*P < 0.05$). *B*: hepatic lipid droplet score comparison after Cav3 vs. GFP gene transfer (n = 7–8; NS, not significant). *C*: hepatic phosphoenolpyruvate carboxykinase (PEPCK) expression by immunoblotting and quantitative RT-PCR. A representative immunoblot is shown in the *inset* (n = 4–5, $^*P < 0.05$). *D*: glucokinase expression by immunoblotting ($n = 4$, NS). *E*: activation of Foxo1 transcriptional factor ($n = 5$, NS). *F*: serum lipid concentrations after Cav3 gene transfer vs. GFP gene transfer in diabetic obese mice (*left*, triglycerides; *right*, cholesterol) ($n = 4$, NS). *G*: histological examination of hepatic tissues. PAS, periodic acid Schiff (PAS) staining of hepatic tissues from mice after Cav3 or GFP gene transfer; diastase-PAS, PAS staining pretreated with diastase.

enzyme, which is regulated by insulin (15). These findings agree with the concept that insulin signals were enhanced in the liver after Cav3 gene transfer. In contrast, the expression of glucokinase (Gck) and Foxo1 activity remained changed (Fig. 3, *D* and *E*).

Abnormal serum lipid concentrations were not improved, potentially because the duration of Cav3 overexpression was short (Fig. 3*F*). Liver triglycerides and serum leptin concentrations were also unchanged (data not shown). Histology and periodic acid-Schiff (PAS) staining demonstrated that the purple staining of glycogen was greater in mice with Cav3 gene transfer (Fig. 3*G*). There was no staining of glycogen when tissues were pretreated with diastase. We also performed oil red O staining and scored the degree of lipid accumulation in hepatic tissues (16). However, there was no significant difference in the lipid score between GFP and Cav3 groups (GFP 1.94 ± 0.34, Cav3 = 2.14 ± 0.25, n = 7–8, P = NS) (Fig. 3*B*).

Similarly, the expression of enzymes involved in lipogenic-related enzymes, such as fatty acid synthase (FAS), sterol regulatory element-binding protein-1, phosphodiesterase 3B, acetyl CoA carboxylase, and liver X receptor, was not significantly different between GFP and Cav3 groups (data not shown).

Cav3 gene transfer improved insulin signals in diabetic obese mice. Cav3 gene injection into diabetic obese mice not only increased the hepatic glycogen content but also improved impaired glucose metabolism. Although Cav3 gene transfer did not alter food intake or body weight (data not shown), impaired glucose tolerance test performance as well as FBG levels (GFP vs. Cav3: 213.3 ± 11.2 vs. 175.3 ± 5.5 mg/dl, n = 8, P < 0.05) were significantly improved (Fig. 4*A*). There was no significant difference in glucose tolerance test performance between non-gene and GFP gene-transferred diabetic obese mice (data not shown). This improvement in glucose metabolism was most likely due to increased insulin action as demonstrated by the improved insulin tolerance test performance (Fig. 4*B*). FBG levels remained lower in mice with Cav3 gene transfer than in control mice with GFP gene transfer, even 90 min after insulin challenge. During the glucose tolerance test, insulin levels were not changed by Cav3 gene transfer (Fig. 4*C*)

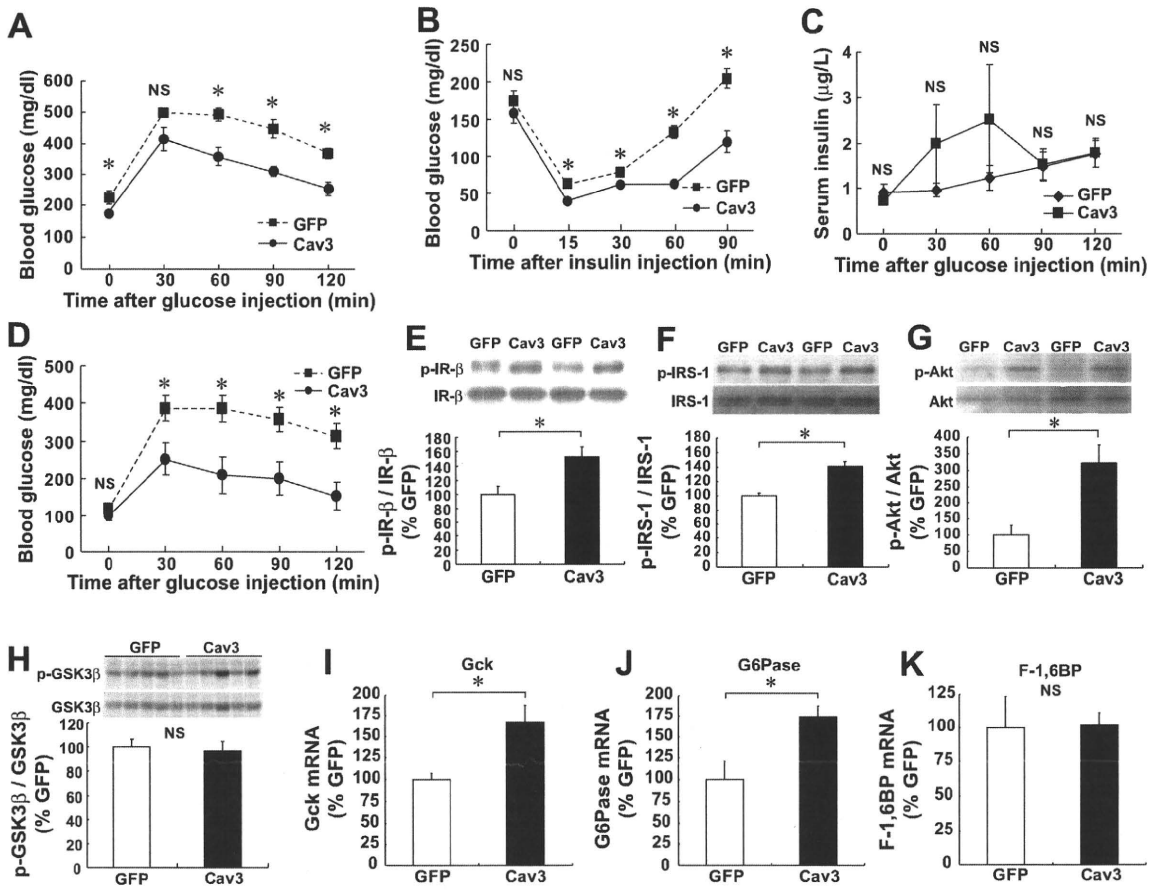

Fig. 4. Cav3 gene transfer improved glucose metabolism in diabetic mice. *A*: glucose tolerance test performance after Cav3 gene transfer and GFP gene transfer in diabetic obese mice (n = 8, *P < 0.05). *B*: insulin tolerance test performance after Cav3 gene transfer vs. GFP gene transfer in diabetic obese mice (n = 4, *P < 0.05). *C*: changes in insulin levels during glucose tolerance test (n = 5, NS). *D*: glucose tolerance test performance in *KKA*^{y} mice (n = 4, *P < 0.05). *E–G*: changes in tissue insulin receptor signals after Cav3 gene transfer. Activation of the molecules involved in insulin receptor signaling, IR-β (*E*), IRS-1 (*F*), and Akt (*G*), after Cav3 gene transfer vs. GFP gene transfer in diabetic obese mice. Representative immunoblots are shown in the *insets* (n = 4–5, *P < 0.05). *H*: changes in GSK3β activity (n = 5, NS). *I–K*: mRNA expression of glucose metabolism-related enzyme in mice liver. Glucokinase (Gck; n = 4–5, *P < 0.05), G6Pase (n = 4–5, *P < 0.05), and F-1,6BP (n = 4–5, NS).

KKA^y mice, which have been widely used as a model of Type 2 diabetes (17), showed only a mild increase in fasting blood glucose concentrations (2), but a marked impairment in glucose tolerance test performance. However, when we injected the Cav3 gene into this mouse model, glucose tolerance test performance was significantly improved (Fig. 4*D*). Therefore, the effect of Cav3 gene transfer on insulin signaling occurs in multiple diabetic mouse models.

Changes in hepatic tissue insulin signaling after Cav3 gene transfer. When whole homogenates of livers from diabetic obese mice with Cav3 gene transfer were examined, we found that IR-β, IRS, and Akt phosphorylation was increased (Fig. 4, *E–G*), suggesting that IR signaling increased after Cav3 gene transfer compared with GFP gene transfer. Because the total protein levels of these molecules including IR-β were not increased, this effect was most likely due to the increased activity of IR-β itself. Because Cav3 gene transfer was restricted to the liver, it was also likely that hepatic Cav3 enhanced the response to insulin, leading to an overall improvement in whole body glucose metabolism. We also examined other relevant enzymes such as Gck, G6Pase, and F-1,6BP (Fig. 4, *I–K*). The mRNA expression of Gck and G6Pase were increased in Cav3 group, suggesting transcriptional activation of these enzymes, while that of F-1,6BP was not changed. The activation of GSK3β was not changed either (Fig. 4*H*).

Cav3 overexpression in hepatic cells. A similar enhancement in insulin signaling by Cav was observed in HepG2 cells, a cultured hepatic cell line. Two days after gene transfer, Cav3 was overexpressed in HepG2 cells to levels equivalent to that of endogenous Cav3 in skeletal muscles (data not shown). IR-β and IRS-1 phosphorylation was significantly enhanced at baseline, which was further increased with increasing concentrations of insulin (0–100 nM) (Fig. 5, *A* and *B*). The maximal activation of IRS-1 was significantly greater in Cav3 gene-transferred cells, suggesting that IR kinase activity in response to insulin was increased by Cav3 overexpression, which confirmed our in vivo observations. At high concentrations (>10 nM), IR-β phosphorylation appeared saturated, while IRS-1 activation was further enhanced in a dose-dependent manner. The cellular content of glycogen was also increased at baseline (Fig. 5*C*). We also examined the phosphorylation of insulin-like growth factor receptors (IGF-1R) in mice with Cav3 gene transfer because IR-β and IGF-1R are structurally similar and Cav3 may alter IGF-1R signaling (14). However, the degree of IGF-1R phosphorylation was similar, suggesting that Cav3 specifically enhances IR-β (Fig. 5*D*).

Caveolin-mediated inhibition of PTP1B activity. The activation of other downstream molecules such as extracellular signal-related kinase (ERK) and phosphatase and tensin homolog (PTEN) in the liver was not significantly different between mice that received Cav3 gene transfer and GFP gene transfer (data not shown). In contrast, it is known that phosphatases, such as PTP1B, can also potently regulate the activity of IR signals (8). In addition, previous studies have demonstrated that PTP1B is present in caveolae (22, 30) and physically interacts with Cav (6). We found that the expression of hepatic PTP1B was significantly increased in diabetic obese mice (Fig. 6*A*) and that overexpressed Cav3 coimmunoprecipitated with PTP1B in the liver (Fig. 6*B*). Furthermore, we found that Cav3 inhibited the activity of PTP1B. A SD-Cav3 peptide, which is known to mimic Cav3 (26), inhibited the activity of purified PTP1B in a dose-dependent manner in vitro, while a similar peptide derived from non-SD Cav3 had no effect (Fig. 6*C*). We also found that a peptide from SD-Cav1 similarly inhibited the activity of PTP1B activity while a NSD-Cav1 had no effect (Fig. 6*D*). These results suggest that Cav3 as well as Cav1 directly interacts with and inhibits the activity of PTP1B. Furthermore, this inhibition may be potentiated in the livers of obese mice where PTP1B expression was increased.

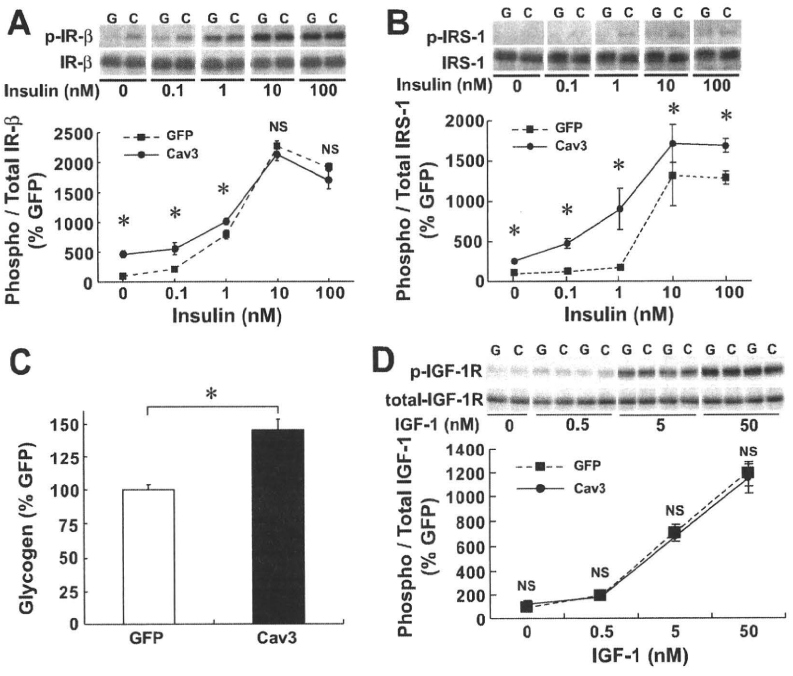

Fig. 5. Cav3 overexpression in HepG2 cells. *A* and *B*: activation of IR-β (*A*) and IRS-1 (*B*) in response to insulin stimulation for 5 min ($n = 5$, $^*P < 0.05$) after Cav3 gene transfer vs. GFP gene transfer. *C*: hepatic glycogen content at baseline after Cav3 gene transfer vs. GFP gene transfer in HepG2 cells ($n = 5$, $^*P < 0.05$). *D*: activation of IGF receptors (IGF-1R) in response to insulin ($n = 4$, NS).

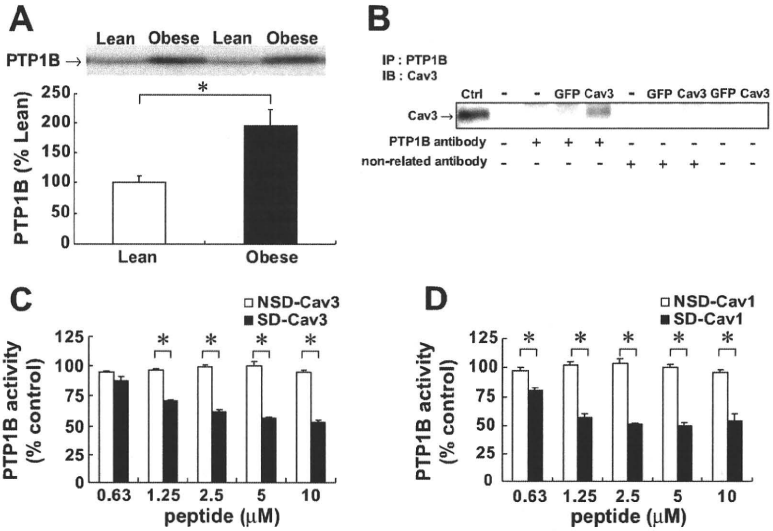

Fig. 6. Caveolin-mediated inhibition of PTP1B activity. *A*: hepatic PTP1B levels by immunoblotting in lean control and obese diabetic mice. A representative immunoblot is also shown ($n = 4$–5, $^*P < 0.05$). *B*: immunoprecipitation assays of PTP1B and Cav3 after Cav3 gene transfer vs. GFP gene transfer in diabetic obese mice. A representative immunoblot is shown. Ctrl, control. *C*: PTP1B activity was determined in the presence of increasing concentrations of scaffolding domain (SD)-Cav3 peptide or nonscaffolding domain (NSD)-Cav3 peptide ($n = 5$, $^*P < 0.05$). *D*: PTP1B activity was determined in the presence of increasing concentrations of SD-Cav1 peptide or NSD-Cav1 peptide ($n = 5$, $^*P < 0.05$).

DISCUSSION

Adenovirus-mediated gene transfer of Cav3 to the liver resulted in increased hepatic glycogen synthesis accompanied by decreased hepatic PEPCK protein levels. Insulin sensitivity, as measured by changes in FBG levels upon insulin injection and glucose tolerance test performance, were improved after Cav3 gene transfer in obese diabetic mice. A similar improvement in glucose metabolism was observed in *KKA*^{y} mice. Overexpression of Cav3 in cultured hepatic cells led to increased phosphorylation of IR-β and IRS in response to insulin stimulation with increased glycogen synthesis at baseline. Therefore, our findings suggest that Cav enhances insulin signals in the liver. The molecular mechanism of this enhanced insulin action may involve direct stimulation of IR by Cav, because a similar mechanism was previously proposed using purified IR and Cav peptides in vitro (30). Although we do not know the extent of caveolin-mediated inhibition of PTP1B activity in vivo, the physical interaction between PTP1B and caveolin has been reported in other studies (6). Furthermore, several investigators have demonstrated the effect of caveolin peptide administration to regulate signaling activity in cells, suggesting that such interaction of caveolin peptide occurs in living cells as well (4, 12, 25, 31).

Furthermore, as shown in the current study, direct inhibition of PTP1B by Cav may be another mechanism by which Cav enhances insulin signals. Obese diabetic mice showed an upregulation of hepatic PTP1B protein, and PTP1B activity was directly inhibited by a SD-Cav3 peptide. Increased expression of phosphatases in obesity was previously reported for other tissues (1). A physical and functional interaction between Cav and PTP1B might be responsible for the slow recovery of glucose levels in insulin tolerance tests as well as for the marked phosphorylation of IR even at low concentrations of insulin (0–1 nM) in mice with Cav3 gene transfer (Fig. 5*A*). Together, Cav3 gene transfer may be a strategy to improve glucose metabolism in vivo.

Adipose and muscle tissues are the major target organs of insulin action that abundantly express Cav1 and Cav3, respectively. Cav may play an important role in these tissues because disruption of the Cav genes, either Cav1 or Cav3, markedly impairs adipose and muscular insulin signals (7, 22). However, the role of Cav in insulin signals in the liver, another major target organ of insulin action, has been uncertain; the liver does not express abundant levels of Cav but has intact insulin signaling. Our findings have demonstrated that Cav can play an important role in insulin signals in the liver, particularly when overexpressed under pathological conditions, such as insulin resistance induced in diabetics by a high-fat diet.

Cav has been long considered a major inhibitor of growth signals and a tumor growth/proliferation suppressor (29), except in prostate cancer (18). Cav gene therapy has been proposed as a potential treatment to suppress tumor proliferation and/or metastasis in various cancers, such as breast cancer (29). Our findings suggest, however, that Cav3 plays an opposite role in insulin signaling; it stimulates IR activity, leading to enhanced IR signals.

In conclusion, Cav3 may be a conditional but important regulator of glucose metabolism. The lack of Cav impaired insulin sensitivity in adipocytes and muscles where endogenous Cav is abundantly expressed (7, 22). Although the liver does not express high levels of Cav under normal conditions, hepatic insulin signals remain intact. However, when insulin signals are impaired in diabetes, increased Cav expression in the liver improves glucose metabolism. The robust nature of our findings suggests that Cav, a membrane-anchoring protein, enhances IR signals.

ACKNOWLEDGMENTS

We thank Masahiro Sakata for technical assistance.

GRANTS

This work was supported in part by grants from the Ministry of Education, Culture, Sports, Science and Technology of Japan and by the Kitsuen Research Foundation.

DISCLOSURES

No conflicts of interest are declared by the author(s).

REFERENCES

1. **Ahmad F, Azevedo JL, Cortright R, Dohm GL, Goldstein BJ.** Alterations in skeletal muscle protein-tyrosine phosphatase activity and expression in insulin-resistant human obesity and diabetes. *J Clin Invest* 100: 449–458, 1997.
2. **Alberts P, Nilsson C, Selen G, Engblom LO, Edling NH, Norling S, Klingstrom G, Larsson C, Forsgren M, Ashkzari M, Nilsson CE, Fiedler M, Bergqvist E, Ohman B, Bjorkstrand E, Abrahmsen LB.** Selective inhibition of 11 beta-hydroxysteroid dehydrogenase type 1 improves hepatic insulin sensitivity in hyperglycemic mice strains. *Endocrinology* 144: 4755–4762, 2003.
3. **Balbis A, Baquiran G, Mounier C, Posner BI.** Effect of insulin on caveolin-enriched membrane domains in rat liver. *J Biol Chem* 279: 39348–39357, 2004.
4. **Bernatchez PN, Bauer PM, Yu J, Prendergast JS, He P, Sessa WC.** Dissecting the molecular control of endothelial NO synthase by caveolin-1 using cell-permeable peptides. *Proc Natl Acad Sci USA* 102: 761–766, 2005.
5. **Carver LA, Schnitzer JE.** Caveolae: mining little caves for new cancer targets. *Nat Rev Cancer* 3: 571–581, 2003.
6. **Caselli A, Mazzinghi B, Camici G, Manao G, Ramponi G.** Some protein tyrosine phosphatases target in part to lipid rafts and interact with caveolin-1. *Biochem Biophys Res Commun* 296: 692–697, 2002.
7. **Cohen AW, Razani B, Wang XB, Combs TP, Williams TM, Scherer PE, Lisanti MP.** Caveolin-1-deficient mice show insulin resistance and defective insulin receptor protein expression in adipose tissue. *Am J Physiol Cell Physiol* 285: C222–C235, 2003.
8. **Elchebly M, Payette P, Michaliszyn E, Cromlish W, Collins S, Loy AL, Normandin D, Cheng A, Himms-Hagen J, Chan CC, Ramachandran C, Gresser MJ, Tremblay ML, Kennedy BP.** Increased insulin sensitivity and obesity resistance in mice lacking the protein tyrosine phosphatase-1B gene. *Science* 283: 1544–1548, 1999.
9. **Galbiati F, Volonte D, Chu JB, Li M, Fine SW, Fu M, Bermudez J, Pedemonte M, Weidenheim KM, Pestell RG, Minetti C, Lisanti MP.** Transgenic overexpression of caveolin-3 in skeletal muscle fibers induces a Duchenne-like muscular dystrophy phenotype. *Proc Natl Acad Sci USA* 97: 9689–9694, 2000.
10. **Gonzalez E, Nagiel A, Lin AJ, Golan DE, Michel T.** Small interfering RNA-mediated down-regulation of caveolin-1 differentially modulates signaling pathways in endothelial cells. *J Biol Chem* 279: 40659–40669, 2004.
11. **Kawabe J, Okumura S, Lee MC, Sadoshima J, Ishikawa Y.** Translocation of caveolin regulates stretch-induced ERK activity in vascular smooth muscle cells. *Am J Physiol Heart Circ Physiol* 286: H1845–H1852, 2004.
12. **Kwiatek AM, Minshall RD, Cool DR, Skidgel RA, Malik AB, Tiruppathi C.** Caveolin-1 regulates store-operated Ca^{2+} influx by binding of its scaffolding domain to transient receptor potential channel-1 in endothelial cells. *Mol Pharmacol* 70: 1174–1183, 2006.
13. **Lampe MA, Burlingame AL, Whitney J, Williams ML, Brown BE, Roitman E, Elias PM.** Human stratum corneum lipids: characterization and regional variations. *J Lipid Res* 24: 120–130, 1983.
14. **LeRoith D, McGuinness M, Shemer J, Stannard B, Lanau F, Faria TN, Kato H, Werner H, Adamo M, Roberts CT Jr.** Insulin-like growth factors. *Biol Signals* 1: 173–181, 1992.
15. **Liu JS, Park EA, Gurney AL, Roesler WJ, Hanson RW.** Cyclic AMP induction of phosphoenolpyruvate carboxykinase (GTP) gene transcription is mediated by multiple promoter elements. *J Biol Chem* 266: 19095–19102, 1991.
16. **Maislos M, Medvedovskv V, Sztarkier I, Yaari A, Sikuler E.** *Psammomys obesus* (sand rat), a new animal model of non-alcoholic fatty liver disease. *Diabetes Res Clin Pract* 72: 1–5, 2006.
17. **Mauldin JP, Srinivasan S, Mulya A, Gebre A, Parks JS, Daugherty A, Hedrick CC.** Reduction in ABCG1 in Type 2 diabetic mice increases macrophage foam cell formation. *J Biol Chem* 281: 21216–21224, 2006.
18. **Mouraviev V, Li L, Tahir SA, Yang G, Timme TM, Goltsov A, Ren C, Satoh T, Wheeler TM, Ittmann MM, Miles BJ, Amato RJ, Kadmon D, Thompson TC.** The role of caveolin-1 in androgen insensitive prostate cancer. *J Urol* 168: 1589–1596, 2002.
19. **Oka N, Yamamoto M, Schwencke C, Kawabe J, Ebina T, Couet J, Lisanti MP, Ishikawa Y.** Caveolin interaction with protein kinase C: isoenzyme-dependant regulation of kinase activity by the caveolin scaffolding domain peptide. *J Biol Chem* 272: 33416–33421, 1997.
20. **Okumura S, Kawabe J, Yatani A, Takagi G, Lee MC, Hong C, Liu J, Takagi I, Sadoshima J, Vatner DE, Vatner SF, Ishikawa Y.** Type 5 adenylyl cyclase disruption alters not only sympathetic but also parasympathetic and calcium-mediated cardiac regulation. *Circ Res* 93: 364–371, 2003.
21. **Okumura S, Vatner DE, Kurotani R, Bai Y, Gao S, Yuan Z, Iwatsubo K, Ulucan C, Kawabe J, Ghosh K, Vatner SF, Ishikawa Y.** Disruption of type 5 adenylyl cyclase enhances desensitization of cyclic adenosine monophosphate signal and increases Akt signal with chronic catecholamine stress. *Circulation* 116: 1776–1783, 2007.
22. **Oshikawa J, Otsu K, Toya Y, Tsunematsu T, Hankins R, Kawabe J, Minamisawa S, Umemura S, Hagiwara Y, Ishikawa Y.** Insulin resistance in skeletal muscles of caveolin-3-null mice. *Proc Natl Acad Sci USA* 101: 12670–12675, 2004.
23. **Quinn PG.** Inhibition by insulin of protein kinase A-induced transcription of the phosphoenolpyruvate carboxykinase gene. Mediation by the activation domain of cAMP response element-binding protein (CREB) and factors bound to the TATA box. *J Biol Chem* 269: 14375–14378, 1994.
24. **Shiraishi S, Yamamoto R, Yanagita T, Yokoo H, Kobayashi H, Uezono Y, Wada A.** Down-regulation of cell surface insulin receptors by sarco(endo)plasmic reticulum Ca^{2+}-ATPase inhibitor in adrenal chromaffin cells. *Brain Res* 898: 152–157, 2001.
25. **Sukumaran SK, Quon MJ, Prasadarao NV.** *Escherichia coli* K1 internalization via caveolae requires caveolin-1 and protein kinase Calpha interaction in human brain microvascular endothelial cells. *J Biol Chem* 277: 50716–50724, 2002.
26. **Toya Y, Schwencke C, Couet J, Lisanti MP, Ishikawa Y.** Inhibition of adenylyl cyclase by caveolin peptides. *Endocrinology* 139: 2025–2031, 1998.
27. **Varagic VM, Mrsulja BB, Stosic N, Pasic M, Terzic M.** The glycogenolytic and hypertensive effect of physostigmine in the anti-nerve-growth-factor-serum-treated rats. *Eur J Pharmacol* 12: 194–202, 1970.
28. **Williams TM, Cheung MW, Park DS, Razani B, Cohen AW, Muller WJ, Di Vizio D, Chopra NG, Pestell RG, Lisanti MP.** Loss of caveolin-1 gene expression accelerates the development of dysplastic mammary lesions in tumor-prone transgenic mice. *Mol Biol Cell* 14: 1027–1042, 2003.
29. **Williams TM, Lisanti MP.** Caveolin-1 in oncogenic transformation, cancer, and metastasis. *Am J Physiol Cell Physiol* 288: C494–C506, 2005.
30. **Yamamoto M, Toya Y, Schwencke C, Lisanti MP, Myers MG Jr, Ishikawa Y.** Caveolin is an activator of insulin receptor signaling. *J Biol Chem* 273: 26962–26968, 1998.
31. **Zhu L, Schwegler-Berry D, Castranova V, He P.** Internalization of caveolin-1 scaffolding domain facilitated by Antennapedia homeodomain attenuates PAF-induced increase in microvessel permeability. *Am J Physiol Heart Circ Physiol* 286: H195–H201, 2004.

Differential Regulation of Vascular Tone and Remodeling via Stimulation of Type 2 and Type 6 Adenylyl Cyclases in the Ductus Arteriosus

Utako Yokoyama, Susumu Minamisawa, Ayako Katayama, Tong Tang, Sayaka Suzuki, Kousaku Iwatsubo, Shiho Iwasaki, Reiko Kurotani, Satoshi Okumura, Motohiko Sato, Shumpei Yokota, H. Kirk Hammond, Yoshihiro Ishikawa

Rationale: Prostaglandin (PG)E_2, which increases intracellular cAMP via activation of adenylyl cyclases (ACs), induces vasodilation and hyaluronan-mediated intimal thickening (IT) in the ductus arteriosus (DA) during late gestation. After birth, however, differential regulation of vasodilation and IT is preferable for treatment of patients with patent DA and DA-dependent congenital cardiac malformations.

Objective: Our objectives were to examine whether AC isoforms play differential roles in DA vasodilation and IT.

Methods and Results: AC2 and AC6 were more highly expressed in rat DA than in the aorta during the perinatal period. AC6-targeted siRNA counteracted PGE_1-induced hyaluronan production in rat DA smooth muscle cells. Overexpression of AC6 enhanced PGE_1-induced hyaluronan production and induced IT in DA explants. Furthermore, IT of the DA was less marked in mice lacking AC6 than in wild-type and AC5-deficient mice. Stimulation of AC2 attenuated AC6-induced hyaluronan production via inhibition of the p38 mitogen-activated protein kinase pathway and AC6-induced IT of the DA. An AC2/6 activator, 6-[*N*-(2-isothiocyanatoethyl) aminocarbonyl] forskolin (FD1), did not induce hyaluronan-mediated IT in DA explants, although an AC5/6 activator, 6-[3-(dimethylamino)propionyl]-14,15-dihydroforskolin (FD6) did. Moreover, FD1 induced longer vasodilation of the DA than did PGE_1 without significant adverse effects in vivo.

Conclusions: AC6 is responsible for hyaluronan-mediated IT of the DA and AC2 inhibited AC6-induced hyaluronan production. Stimulation of both AC2 and AC6 by FD1 induced longer vasodilation without hyaluronan-mediated IT in the DA in vivo. FD1 may be a novel alternative therapy to currently available PGE therapy for patients with DA-dependent congenital heart disease. (*Circ Res*. 2010;106:1882-1892.)

Key Words: patent ductus arteriosus ■ prostaglandins ■ smooth muscle ■ vasodilation ■ remodeling

Prostaglandin (PG)E_2 and PGE_1 play principal roles in maintaining the patency of the ductus arteriosus (DA) during gestation. PGE_1 is widely used to keep the DA open in patients with DA-dependent congenital heart diseases, because both PGE_1 and PGE_2 increase the intracellular concentration of cAMP, resulting in vasodilation in the DA.[1,2] On the other hand, we have demonstrated that PGE-EP4-cAMP signals during late gestation increased hyaluronan production in the DA and consequently induced intimal thickening (IT), which is critical for permanent closure of the DA after birth.[3] Therefore, the effects of $PGE_{1/2}$ on vasodilation and remodeling oppose each other in terms of regulation of the DA after birth. Differential regulation of vasodilation and IT in the DA would be preferable for patients who need PGE/anti-PGE therapy.

Because intracellular cAMP is synthesized by adenylyl cyclases (ACs), which are transmembrane enzymes activated by G protein-coupled receptors, including PGE receptors, ACs must play an important role in regulating vasodilation and remodeling in the DA. To date, nine different isoforms of membrane-bound forms of ACs (AC1 through AC9) have been identified in vertebrate tissues.[4] Most tissues express several AC isoforms, which exhibit remarkable diversities in their biochemical properties.[5,6] Because smooth muscle cells

Original received December 13, 2009; revision received April 12, 2010; accepted April 15, 2010.

From the Cardiovascular Research Institute (U.Y., A.K., S.S., R.K., S.O., M.S., Y.I.), the Department of Pediatrics (S.I., S.Y.), Yokohama City University Graduate School of Medicine, Japan; the Department of Life Science and Medical Bioscience (S.M.), Waseda University Graduate School of Advanced Science and Engineering, Tokyo, Japan; VA San Diego Healthcare System (T.T., H.K.H.), San Diego, Calif; the Department of Medicine (T.T., H.K.H.), University of California San Diego, La Jolla; the Cardiovascular Research Institute, Departments of Cell Biology & Molecular Medicine and Medicine (Cardiology) (K.I.,Y.I.), New Jersey Medical School, University of Medicine & Dentistry of New Jersey, Newark.

Correspondence to Susumu Minamisawa, Department of Life Science and Medical Bioscience, Waseda University Graduate School of Advanced Science and Engineering, 2-2, Wakamatsu-cho, TWIns, Shinjuku-ku, Tokyo 162-8480, Japan (E-mail sminamis@waseda.jp); or to Yoshihiro Ishikawa, the Cardiovascular Research Institute, Yokohama City University Graduate School of Medical Science, Yokohama 236-0004, Japan (E-mail yishikaw@yokohama-cu.ac.jp).

Circulation Research **is available at http://circres.ahajournals.org** **DOI: 10.1161/CIRCRESAHA.109.214924**

(SMCs) in the DA exert biological properties distinct from SMCs in other vessels such as the aorta, we hypothesized that such properties are attributable, at least in part, to the distinct roles of specific AC isoforms in the DA.

In addition to the role of $PGE_{1/2}$ in vasodilation, the PGE-AC-cAMP signal cascade has been shown to regulate vascular remodeling.[7,8] For example, cAMP markedly inhibits proliferation of SMCs[9] and reduces IT after arterial injury in vivo,[10] a process that shares many aspects with IT in the DA.[1,11] Interestingly, several studies have demonstrated that $PGE_{1/2}$ inhibits the proliferation of vascular SMCs,[7,8] whereas others have reported that PGE_2 stimulates the growth of vascular SMCs.[12,13] Such diversities in the effects of PGE signaling might be related to differential expression of AC isoforms among vascular tissues. It has been difficult, however, to evaluate the contribution of ACs to relevant phenomena in an AC isoform-dependent manner, because multiple isoforms of ACs are coexpressed. This is partially attributable to the lack of available AC isoform-selective pharmacological regulators. In previous studies, we synthesized more than 200 new derivatives of forskolin (a non–isoform-selective AC activator) and identified derivatives that are selective to specific AC isoforms.[6,14,15] Such AC isoform-selective activators enable us to explore the role of each AC isoform in vascular tone and remodeling especially in vivo. In the present study, using such AC isoform-specific activators, overexpression or selective silencing of AC isoforms and AC-isoform deficient-mice, we have investigated the role of AC isoforms and the availability of AC isoform-selective activators in regulating DA vascular tone and remodeling.

Non-standard Abbreviations and Acronyms

AC	adenylyl cyclase
Adv	adenovirus-mediated gene transfer
DA	ductus arteriosus
E	embryonic day
ERK	extracellular signal-related kinase
FD1	6-[*N*-(2-isothiocyanatoethyl) aminocarbonyl] forskolin
FD6	6-[3-(dimethylamino)propionyl]-14,15-dihydroforskolin
HAS2	hyaluronan synthase type 2
IT	intimal thickening
JNK	c-Jun N-terminal kinase
KO	knockout
MAPK	mitogen-activated protein kinase
PGE	prostaglandin E
PK	protein kinase
siRNA	small interfering RNA
SMC	smooth muscle cell

Methods

An expanded Methods section is available in the Online Data Supplement at http://circres.ahajournals.org.

Reagents

Forskolin derivatives: 6-[*N*-(2-isothiocyanatoethyl) aminocarbonyl] forskolin (FD1),[14,16] and 6-[3-(dimethylamino)propionyl]-14,15-dihydroforskolin (FD6)[14] were kindly provided by Nippon Kayaku Co, Ltd (Tokyo, Japan).

Animals and Tissues

All animals were cared for in compliance with the guiding principles of the American Physiological Society. The experiments were approved by the ethical committee of animal experiments at Yokohama City University School of Medicine. Wistar rat embryos were obtained from timed-pregnant mothers (Japan SLC Inc, Shizuoka, Japan). Pooled tissues of DA and aorta were obtained from rat embryos on embryonic day (E)19 (n>60) and E21 (n>60) and neonates on the day of birth (day0, n>60). Generation and phenotypes of AC5 knockout mice (AC5KO) and AC6 knockout mice (AC6KO) have been described previously.[17,18] All mice were littermates from heterozygote crosses.

Isolation and Culture of Rat Ductus Arteriosus Smooth Muscle Cells

Vascular SMCs were obtained from DA and aorta of Wistar rat embryos at E21 as previously described.[19]

Quantitative and Semiquantitative RT-PCR

Isolation of total RNA and generation of cDNA were performed and RT-PCR analysis was done as previously described.[19] The primers were designed based on the rat nucleotide sequences of AC isoforms. Each primer set was designed between multiple exons (Online Table I), and PCR products were confirmed by sequencing. The abundance of each gene was determined relative to the GAPDH transcript using TaqMan Rodent GAPDH control reagents kits (Applied Biosystems, Foster City, Calif).

Immunoblot Analysis

Proteins from whole cells were analyzed by immunoblotting as previously described.[19]

RNA Interference

Double-stranded small interfering (si)RNAs to the selected regions of AC2–7 and the negative siRNA used as a control were purchased from QIAGEN (Hilden, Germany) or Invitrogen (San Diego, Calif) (Online Table II). According to the instructions of the manufacturer, cells were transfected with siRNA (300 pmol), using Lipofectamin RNAiMAX (Invitrogen).

Adenovirus Construction

Full-length cDNA-encoding rat AC2 was cloned into the shuttle vector for construction of an adenoviral vector harboring AC2 through the use of an AdenoX adenovirus construction kit (Clontech, Tokyo, Japan). Adenovirus encoding murine AC6 driven by a cytomegalovirus promoter was generated by homologous recombination as previously described.[20] Adenovirus encoding MKK3 was kindly provided by Dr Yibin Wang (University of California, Los Angeles).[21]

cAMP Production by Radioimmunoassay

Rat ductus arteriosus smooth muscle cells (DASMCs) were serum-starved for 48 hour and assayed for cAMP production by RIA after incubation with drugs of interest (Online Data Supplement).

Quantitation of Hyaluronan

The amount of hyaluronan in the cell culture supernatant was measured by the latex agglutination method as previously described.[3]

Organ Culture

DA organ culture was performed as previously described.[3,22]

Measurement of Isometric Tension of the Vascular Rings of DA

Isometric tension of the vascular rings of DA was measured as previously described.[23]

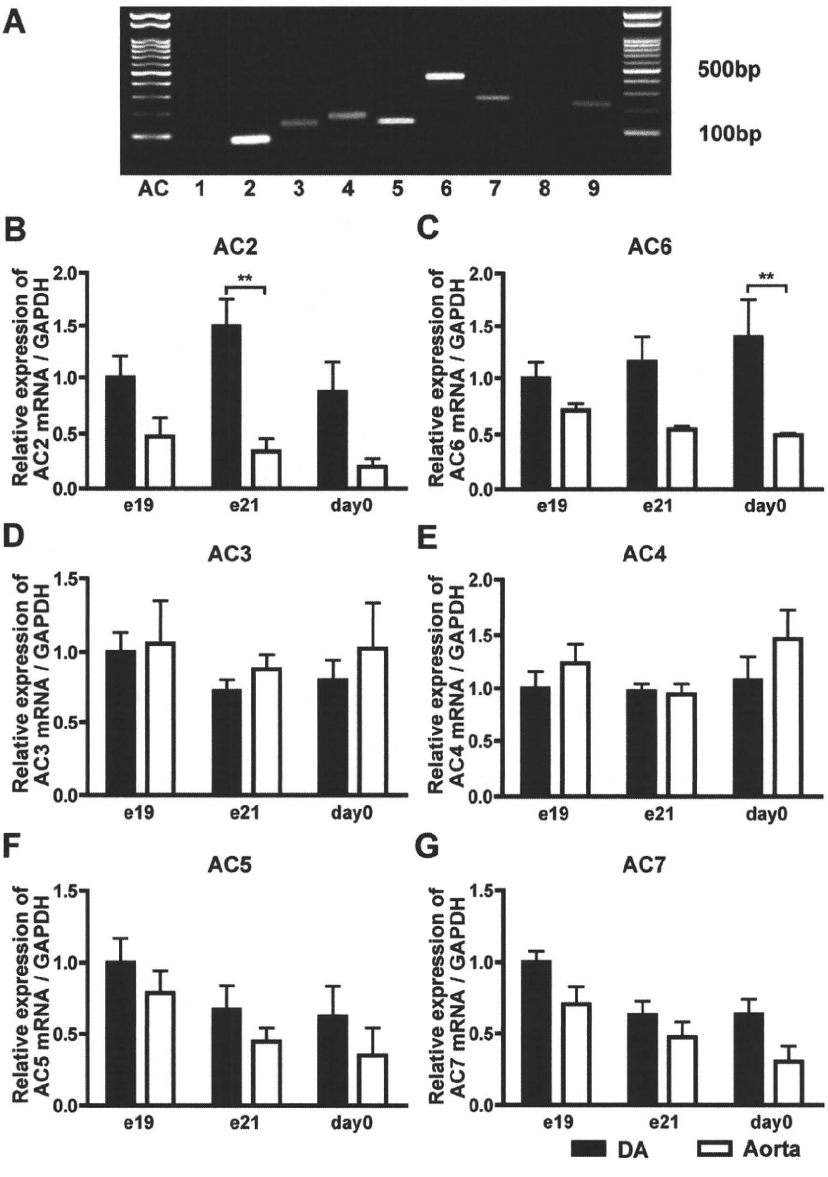

Figure 1. Multiple transcripts of AC isoforms in rat DA. A, mRNA expression of AC isoforms using semiquantitative RT-PCR in rat E21 DA. **B through G,** Quantitative RT-PCR analyses of AC2–7. $^{**}P<0.01$. Data are from 6 independent experiments.

Rapid Whole-Body Freezing Method

To study the in situ morphology and inner diameter of neonatal DA, a rapid whole-body freezing method was used as previously described.[24] The fetuses at E21 were delivered by cesarean section and intraperitoneally injected 1 hour after birth with PGE_1, FD1 or FD6 in 200 μL of saline. The minimal dose of FD1 (10.8 mg/kg of body weight) and FD6 (1.29 mg/kg of body weight) that caused maximal dilation in the DA were used.

Protein Kinase A Activity

Protein kinase (PK)A activity was measured using an assay kit (StressGen Biotechnologies, Ann Arbor, Mich) according to the instructions of the manufacturer, as described previously.[25]

Statistical Analysis

Data are shown as the means±SEM of independent experiments. Statistical analysis was performed between two groups by unpaired Student t test or between multi-groups by one-way ANOVA followed by Student–Newman–Keuls multiple comparison test. A value of $P<0.05$ was considered significant.

Results

Multiple Transcripts of AC Isoforms in Rat DA

First, we detected all isoforms except for AC1 and AC8 in rat E21 DA by semiquantitative analyses (Figure 1A). Next, quantitative RT-PCR analyses of AC2–7 showed that AC2, AC5, and AC6 were abundantly expressed in rat DA and that the expression levels of AC2 and AC6 were significantly higher in the DA than in the aorta during the perinatal period, whereas those of AC5 were comparable between the DA and the aorta. The expression of AC2 reached maximal level in E21 DA (Figure 1B), whereas that of AC6 was increased during development in rat DA (Figure 1C).

AC6 Is Responsible for Hyaluronan Production in DASMCs

We examined the contribution of AC2, AC5 and AC6 to PGE_1-induced cAMP production in DASMCs by using AC2-,

AC5-, and AC6-targeted siRNAs. The expression levels of ACs mRNAs using the siRNAs are shown in Online Figure I. Silencing of AC5 or AC6 dramatically decreased PGE_1-induced cAMP production and that of AC2 also decreased PGE_1-induced cAMP production by 58% (Figure 2A), indicating that AC2, AC5 and AC6 are major isoforms responsible for cAMP production by PGE_1 in DASMCs. We then examined the effect of ACs on hyaluronan production in DASMCs. AC6-targeted siRNA weakened PGE_1-induced hyaluronan production, whereas AC2-, and AC5-targeted siRNA did not (Figure 2B). Neither AC3-, AC4-, nor AC7-targeted siRNA weakened PGE_1-induced hyaluronan production (Online Figure II). Using adenovirus-mediated gene transfer of AC2 and AC6 (Adv.AC2 and Adv.AC6), efficacy of which is shown in Online Figure III, we found that the overexpression of AC6, but not of AC2, further enhanced PGE_1-induced hyaluronan production when compared with the overexpression of LacZ as a control (Figure 2C). Interestingly, co-overexpression of both AC2 and AC6 negated AC6-mediated enhancement of hyaluronan production.

AC6 Gene Transfer, but Not AC2, Promoted IT in Rat DA Explants

When AC6 was overexpressed in immature rat DA explants in which IT had not yet formed, prominent IT with strong hyaluronan deposition was observed in AC6-overexpressed DA explants, as compared to LacZ controls (Figure 3A, 3B, and 3D). The internal lumen of the DA treated with Adv.AC6 was almost completely closed (Figure 3C). However, overexpression of AC2 did not promote hyaluronan deposition and IT formation. Further, Adv.AC2 abrogated AC6 overexpression-induced hyaluronan production and IT ex vivo, which is consistent with the data in Figure 2C. Taken together, these results indicate that AC2 has an inhibitory effect on AC6-induced hyaluronan-mediated IT in DA explants.

AC6 Deficiency Decreased IT in Mouse DA

Although AC5 and AC6 share an extremely high amino acid homology, the above experiments suggested that AC6 is a major isoform for DA remodeling. We therefore examined whether AC6 indeed plays a major role in in vivo IT of the DA and found that genetic disruption of the AC6 isoform resulted in less IT during late gestation (E18.5) (Figure 4B, 4D, and 4F). It should be noted that DAs closed after birth in AC6KO mice (data not shown). The IT of AC5KO mice was normally developed at E18.5 (Figure 4A, 4C, and 4E), and the DA of AC5KO mice closed after birth (data not shown). These findings support the conclusion that AC6 plays a primary role in IT and, thus, the vascular remodeling in the mouse DA.

Effect of Isoform-Selective AC Activators on cAMP Accumulation in Rat DASMCs

Based on the findings of previous crystallographic studies and computer-assisted drug design, we identified forskolin derivatives (FD1 or FD6) that have enhanced selectivity for AC2 or AC5 in regulating tissue AC catalytic activity.[14]

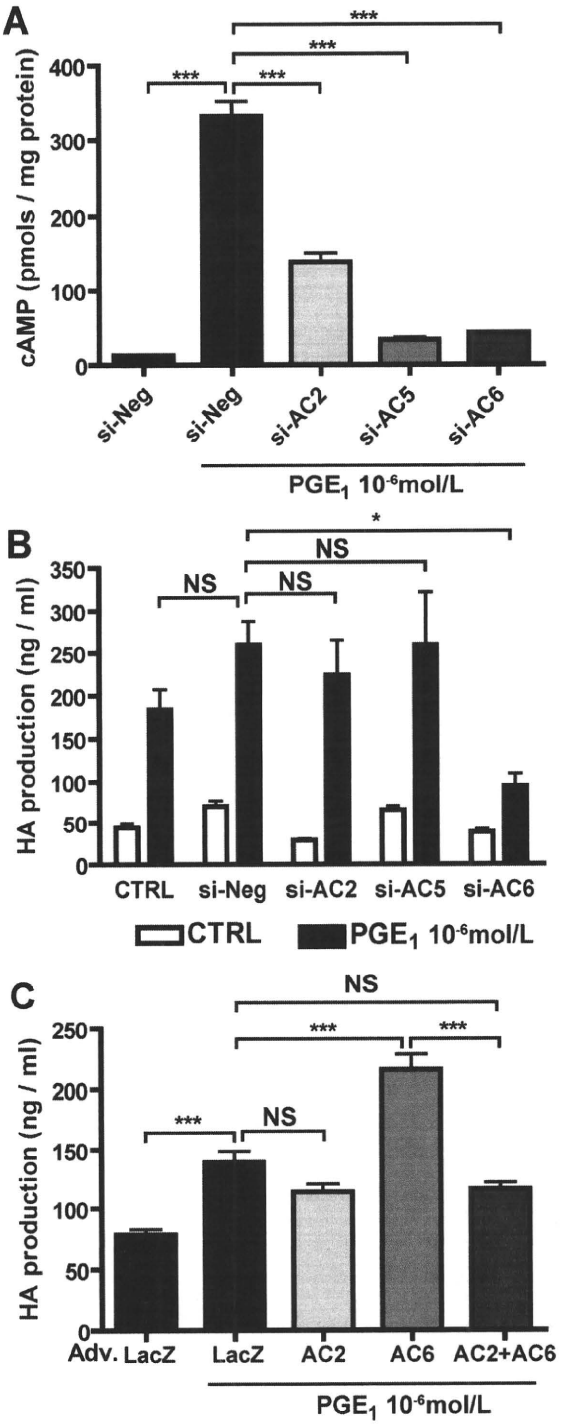

Figure 2. AC6 is responsible for hyaluronan production in DASMCs. A, PGE_1 induced cAMP accumulation in DASMCs in the cells treated with negative siRNA. AC2-, AC5-, and AC6-targeted siRNA decreased PGE_1-induced cAMP production (n=4). **B,** AC6-targeted siRNA attenuated PGE_1-induced hyaluronan (HA) production, whereas AC2- and AC5-targeted siRNA did not (n=7 to 11). **C,** Adv.AC6 enhanced PGE_1-induced hyaluronan production. Adv.AC2 abolished the Adv.AC6-induced enhancement of hyaluronan production (n=4). $^*P<0.05$ and $^{***}P<0.001$. NS indicates not significant.

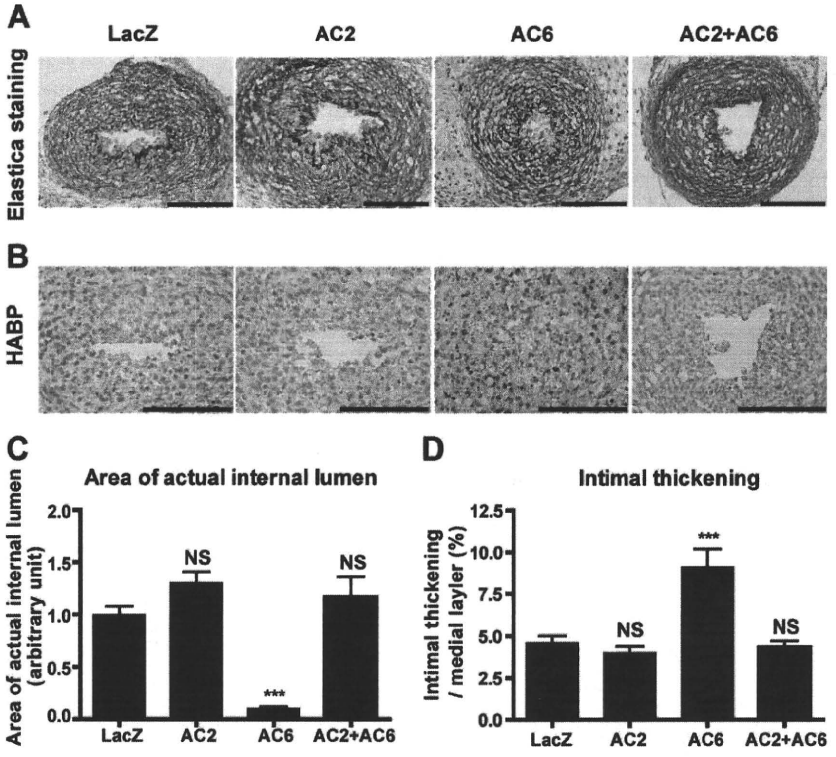

Figure 3. Adenovirus-mediated AC6 gene transfer promoted IT in rat DA explants. A, Elastica van Gieson staining for cultured DA explants overexpressed with Adv.LacZ, Adv.AC2, Adv.AC6, or Adv.AC2+Adv.AC6. **B,** Strong immunoreaction to hyaluronan in DA explants cultured with Adv.AC6. **Bars:** 100 μm. **C,** The area of the internal lumen of the DA treated with Adv.AC6 was significantly decreased (n=8 to 9). **D,** The ratio of IT to the thickness of the medial layer was increased in the DA treated with Adv.AC6, but not with Adv.AC2 (n=8 to 9). ***$P<0.001$. HABP indicates hyaluronan-binding protein.

However, the ability of cAMP production via AC6 of FD1 and FD6 has not been demonstrated. FD1 enhanced LacZ control-induced cAMP accumulation in DASMCs infected with Adv.AC2 or Adv.AC6 (Figure 5A). FD6 enhanced cAMP accumulation in DASMCs with Adv.AC6, but not with Adv.AC2. These data suggest that FD1 stimulates both AC2 and AC6 and that FD6 stimulates AC5 and AC6. We confirmed that FD1 (AC2/6 stimulator) and FD6 (AC5/6 stimulator) increased cAMP accumulation in DASMCs in a dose-dependent manner (Figure 5B).

The Effects of Isoform-Selective AC Activators on DASMC Hyaluronan Production

We then found that FD6 significantly increased hyaluronan production (Figure 5C) and transcripts of hyaluronan synthase type 2 (HAS2) in DASMCs at 10^{-5} mol/L (Figure 5D). In contrast, FD1, in doses up to $10^{-5.5}$ mol/L, did not increase hyaluronan production or HAS2 transcripts up. It should be noted that production of cAMP by FD1 at a concentration of $10^{-5.5}$ mol/L was equivalent to that by FD6 at 10^{-5} mol/L (Figure 5B and 5C) and that FD1 significantly decreased DASMC viability at a concentration higher than 10^{-5} mol/L. Silencing of AC6, but not of AC5, abolished FD6-induced hyaluronan production (Figure 5E), indicating that AC6 is responsible for FD6-induced hyaluronan production. Furthermore, to examine whether the effect of FD6 on hyaluronan production is specific to DASMCs, we found that FD6 did not induce hyaluronan production in SMCs from the rat aorta (Figure 5F), because expression of AC6 mRNA in aortic SMCs was approximately 60% lower than in DASMCs. However, when AC6 was overexpressed in the aortic SMCs, hyaluronan production was significantly increased by 1.4±0.1-fold (n=6) in the presence of FD6 (10^{-5} mol/L), suggesting that this data can provide insight into a more general vascular remodeling by AC6.

Involvement of MKK3-p38 MAPK in AC6-Induced Hyaluronan Production

To examine the mechanism by which AC2 inhibits AC6-induced hyaluronan production, we focused on several signal pathways such as p38 mitogen-activated protein kinase (MAPK). We found that FD6 increased phosphorylation of p38 protein in DASMCs, whereas FD1 and N6-Benzoyladenosine-cAMP (Bnz-cAMP), a PKA selective cAMP analog, did not (Figure 6A and 6B). FD6-induced phosphorylation of p38 and MKK3/6 was negated in DASMCs treated with AC6-targeted siRNA (Figure 6C). FD1 increased phosphorylation of p38 and MKK3/6 when AC2 expression was downregulated by AC2-targeted siRNA (Figure 6C). FD6-induced hyaluronan production was attenuated by SB203580, a p38 inhibitor, or H89, a PKA inhibitor. Combined treatment of SB203580 and H89 further inhibited hyaluronan production (Figure 6D). In contrast, SB203580 did not affect PKA-induced hyaluronan production (Figure 6E). These data suggest that p38 MAPK and PKA independently regulate hyaluronan production. Furthermore, overexpression of MKK3, the efficacy of which is demonstrated by Adv.MKK3 (Figure 6F), enhanced FD6-induced hyaluronan production in DASMCs (Figure 6G). Extracellular signal-related kinase (ERK)1/2 and c-Jun N-terminal kinase (JNK) were not phosphorylated by FD6 (data not shown). Phospholipase C, PKC, IP3 receptor, PI3-kinase, and Epac signaling were not

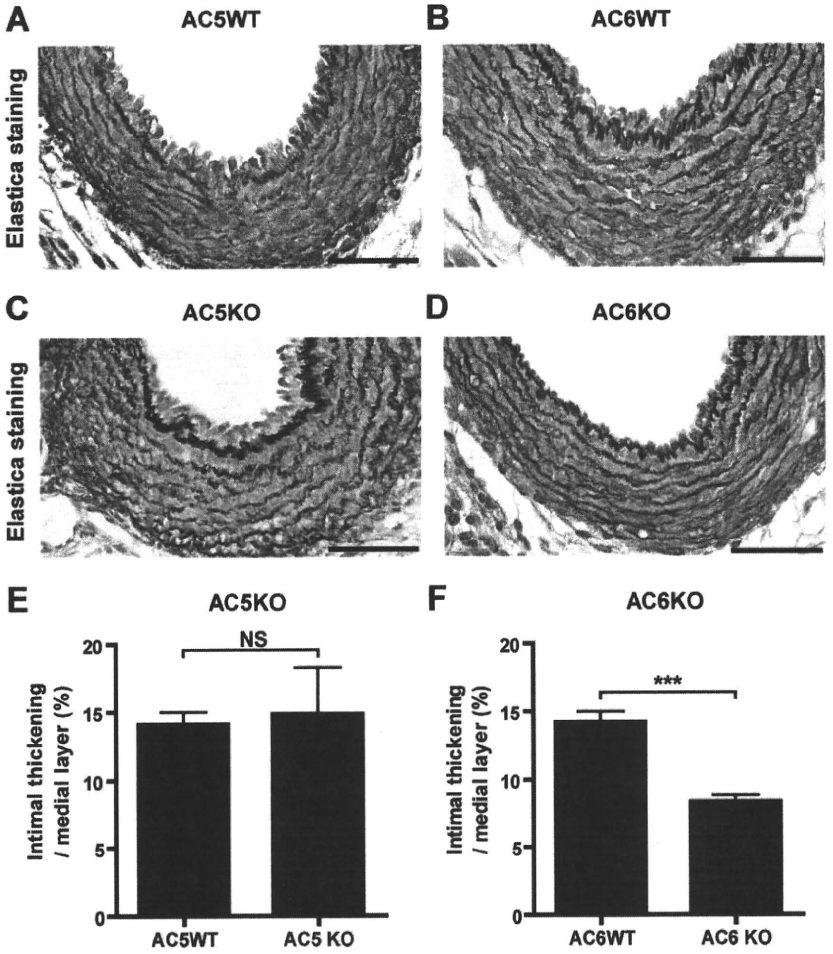

Figure 4. Impaired IT in the mouse DA attributable to AC6, but not AC5, deficiency. A, C, and E, DAs from AC5KO mice at E18.5 were stained with elastica van Gieson stain. Both AC5KO and wild-type (WT) mice showed IT in the DA (n=4 to 5). **B, D, and F,** DAs from AC6KO mice at E18.5 had less IT compared to wild-type mice (n=8). **Bars:** 50 μm. ***$P<0.001$.

involved in AC6-induced hyaluronan production, as shown using specific agonists or inhibitors for each pathway (Online Figure IV). These data indicate that stimulation of AC6 promotes hyaluronan production via both p38 and PKA pathways and that AC2 inhibits the AC6-activated MKK3-p38 pathway.

The Effects of Isoform-Selective AC Activators on IT Ex Vivo

We then examined the effects on FD1 and FD6 on IT using DA explants. Consistent with other data (Figures 5 and 6), 48 hour incubation with FD6 significantly induced IT, increased hyaluronan production, and narrowed the internal lumen in DA explants (Figure 7). It should be noted that FD1 and FD6, similarly to forskolin and PGE_1, inhibited proliferation of DASMCs. Overexpression of AC2 or AC6 also inhibited DNA synthesis in DASMCs (Online Figure V), indicating that FD6 does not directly promote IT by proliferation of DASMCs.

The Effects of Isoform-Selective AC Activators on Vasodilation

Because $PGE_{1/2}$ strongly dilates the DA via activation of ACs, AC activators should be potent vasodilators for the DA as well. We found that FD1 and FD6 similarly attenuated indomethacin-induced contraction in DA explants (Figure 8A). We then examined the vasodilatory effect of FD1 and FD6 in vivo using a whole-body freezing method. Here, the DA closed completely 1 hour after birth (Figure 8B) when PGE_1, FD1, or FD6 were administrated by intraperitoneal injection. Consistent with previous data,[24] PGE_1 caused maximal dilatation 30 minutes after injection and then the DA completely closed within 2 hour (Figure 8C and 8D). FD1 induced maximal dilatation of the DA up to 4 hour and then the DA gradually contracted, suggesting that FD1 has a longer vasodilatory effect on the DA than dose PGE_1. Although FD6 also dilated the DA 30 minutes after injection, all neonates died approximately 4 hours after injection because of suppression of respiration, which is the same side effect caused by PGE_1 and was not caused by FD1. We also found that FD1 and FD6 did not affect the diameter of the ascending aorta, whereas FD6, but not FD1, significantly dilated the main pulmonary artery up to 4 hour after administration (Online Figure VI, A through C). Using cultured DASMCs, AC6-targeted siRNA attenuated forskolin-induced phosphorylation of vasodilator-stimulated phosphoprotein (VASP), whereas AC2-targeted siRNA had no effect, suggesting that AC6 is primarily involved in DA vasodilation (Online Figure VI, D).

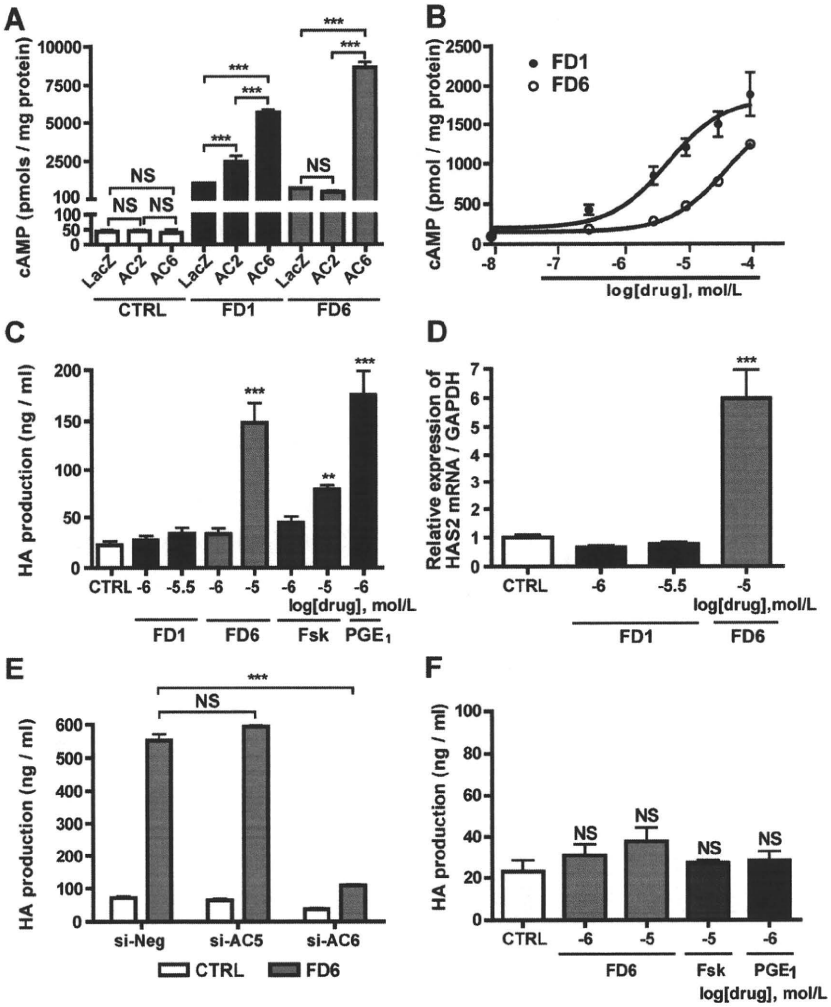

Figure 5. The effects of FD1 and FD6 on cAMP and hyaluronan production in DASMCs. A, Effect of overexpression of AC2 or AC6 on FD1- or FD6-induced cAMP accumulation (n=6). **B,** FD1 and FD6 increased cAMP accumulation in DASMCs in a dose-dependent manner (n=4). **C,** FD6, but not FD1, increased hyaluronan production (n=8 to 11). **D,** FD6 significantly increased HAS2 mRNA (n=6). **E,** AC6-targeted siRNA negated FD6-induced hyaluronan production (n=4). **F,** FD6, PGE_1, and forskolin did not induce hyaluronan production in aortic SMCs (n=6). $^{**}P<0.01$ and $^{***}P<0.001$ vs control (CTRL). Fsk indicates forskolin.

Taken together, these results reveal that AC6 play a primary role in hyaluronan-mediated vascular remodeling in the DA through activation of the PKA and MKK3-p38 MAPK pathways and that AC2 has an inhibitory effect on AC6-mediated hyaluronan production and IT.

Discussion

The Effect of AC2, AC5, and AC6 on Vascular Remodeling

The present study demonstrated for the first time that AC plays a significant role in vascular remodeling in the DA. Intimal thickening during development is a critical form of vascular remodeling for postnatal closure of the DA.[3,26] We found that hyaluronan induced by PGE-EP4-cAMP signaling is a prominent constituent of the extracellular matrix of IT in the DA.[3] It seems a worthwhile endeavor to investigate mechanisms leading to an increase in hyaluronan, because insights into its regulatory mechanisms and signaling pathways might eventually lead to ways of controlling hyaluronan-mediated IT in the DA. However, the isoform-selective role of AC in DA vascular remodeling has not previously been reported. Importantly, we found that AC6 is responsible for hyaluronan-mediated IT in the DA via activation of the MKK3-p38 and PKA pathways and that AC2 has an inhibitory effect on AC6-mediated hyaluronan production and DA remodeling. We also demonstrated that simultaneous stimulation of AC2 and AC6 by FD1 produces a longer vasodilatory effect than does PGE_1 without inducing hyaluronan-mediated IT.

It is important to identify whether the source of hyaluronan is from SMCs or endothelial cells of the DA. Using cell sorting analysis, we found that the expression levels of HAS1, HAS2 and AC6 mRNAs in CD31-positive/CD45-negative endothelial cells from E21 rat DA were significantly lower than those in CD31-negative/CD45-negative SMCs from E21 rat DA (Online Figure VII). Therefore, we believe that DASMCs are a major source of hyaluronan production.

DA IT in AC6-Deficient Mice

Our results also showed that the DA of AC6KO mice had less fully formed IT during late gestation. These results support the belief that AC6 plays a role in EP4-mediated hyaluronan synthesis. Nevertheless, the DA of AC6KO mice eventually closed after birth, similarly to wild-type mice, whereas the DA remained open in EP4KO mice. These results suggest

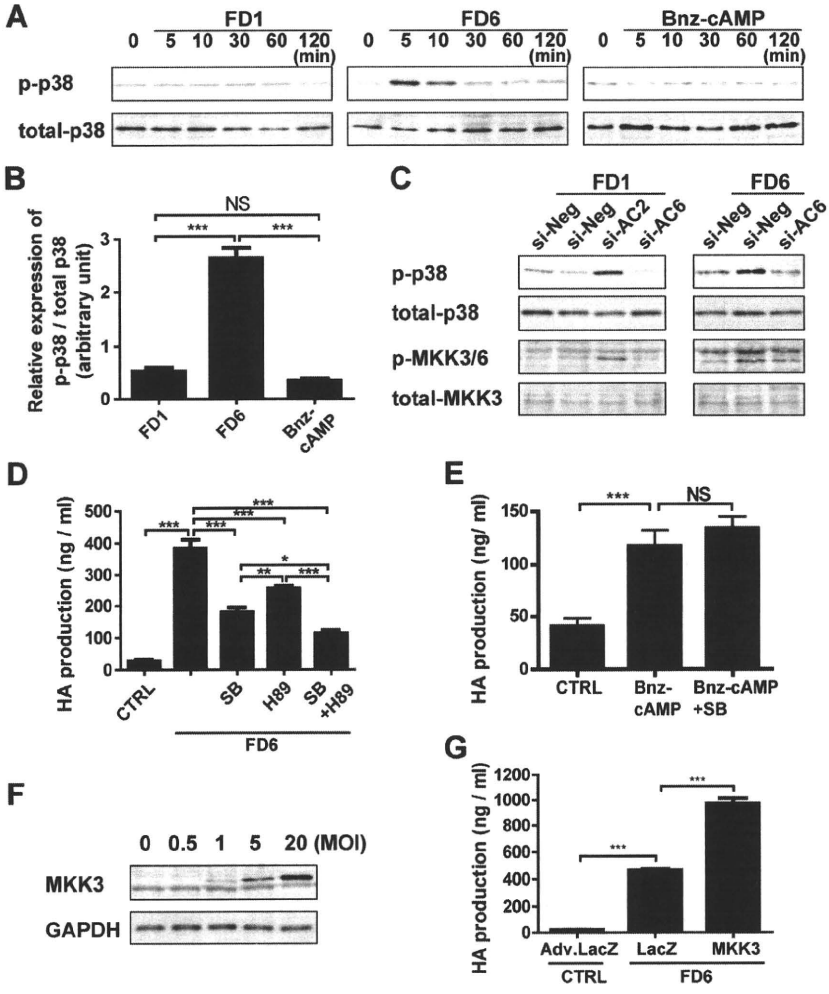

Figure 6. The signaling pathway of AC6-induced hyaluronan production in DASMC. A, Phosphorylation of p38 protein (p-p38) by FD1 ($10^{-5.5}$ mol/L), FD6 (10^{-5} mol/L), or Bnz-cAMP (10^{-5} mol/L) (n=4). **B,** Quantification of the ratio of p-p38 to total p38 after 5 minutes stimulation by FD1, FD6 or BnzcAMP. (n=4). **C,** Phosphorylation of p38 and MKK3/6 induced by 5 minutes treatment of FD1 ($10^{-5.5}$ mol/L) or FD6 (10^{-5} mol/L) in DASMCs treated with si-negative, si-AC2, or si-AC6 RNA (n=4). **D,** FD6-induced hyaluronan production was attenuated by SB203580 (SB) (2×10^5 mol/L) and H89 (10^6 mol/L) (n=6). **E,** SB203580 (2×10^5 mol/L) did not affect Bnz-cAMP-induced hyaluronan production (n=6). **F,** MKK3 protein expression by Adv.MKK3. MOI indicates multiplicity of infection. **G,** Adv.MKK3 enhanced FD6-induced hyaluronan production (n=6). *$P<0.05$, **$P<0.01$, ***$P<0.001$.

that other AC isoforms might compensate for deficiency of AC6. Alternatively, other EP4 signal pathways in addition to the AC-cAMP pathway may be involved in the patency of EP4KO mice. Further study is required to determine how multiple signaling pathways contribute to yield IT in the DA. We assume that the closure of the DA in AC6KO mice may be delayed after birth because of insufficient IT, which will also be addressed in our future studies.

Interaction of AC2 and AC6 Signaling in Hyaluronan-Mediated IT

AC isoforms have specific patterns of regulation by G proteins, protein kinases and calcium/calmodulin. For example, cAMP production by AC2 is stimulated by several signals including G_s-α and $\beta\gamma$-subunits, and by PKC. In contrast, cAMP production by AC6 is only stimulated by G_s-α and inhibited by G_i-α, PKA, and low concentrations of Ca^{2+}.[4,27] Moreover, different AC isoforms have different effects on cAMP-mediated responses independent of their rate of synthesis of cAMP.[28] To the best of our knowledge, this is the first study to show how the effect of an AC isoform counteracts the effect of another isoform independent of cAMP production. We demonstrated that overexpression of AC2 by itself has little effect on hyaluronan production and appears to have an inhibitory effect on AC6-induced hyaluronan and IT. These data are consistent with the other experiments in which activation of both AC2 and AC6 by FD1 did not induce hyaluronan and IT in DASMCs and DA explants. The response of FD6 to hyaluronan production was much greater than that of FD1, even though FD6 produced less cAMP than FD1 at the same concentrations, suggesting that this process is not simply dependent on the amount of intracellular cAMP.

The next important question is the mechanism how AC2 and AC6 differentially regulate vascular remodeling of the DA. Our results demonstrated that AC6 induced hyaluronan production via the MKK3-p38 MAPK and PKA pathways and that AC2 inhibited the MKK3-p38 pathway, resulting in inhibition of AC6-induced hyaluronan production. PKC, phospholipase C, PI3-kinase, Epac, and other MAPK pathways including ERK and JNK were not involved in AC6-induced hyaluronan production. In addition, we also found that AC2 is primarily localized in the caveolae fraction, whereas AC5/6 localized in the caveolae and the noncaveolae fractions (Online Figure VIII). This differential localization may change the effect of AC2 and AC6 on the downstream signal pathways. Identification of the upstream target linking AC6 and the MKK3-p38 pathways will be addressed in future studies.

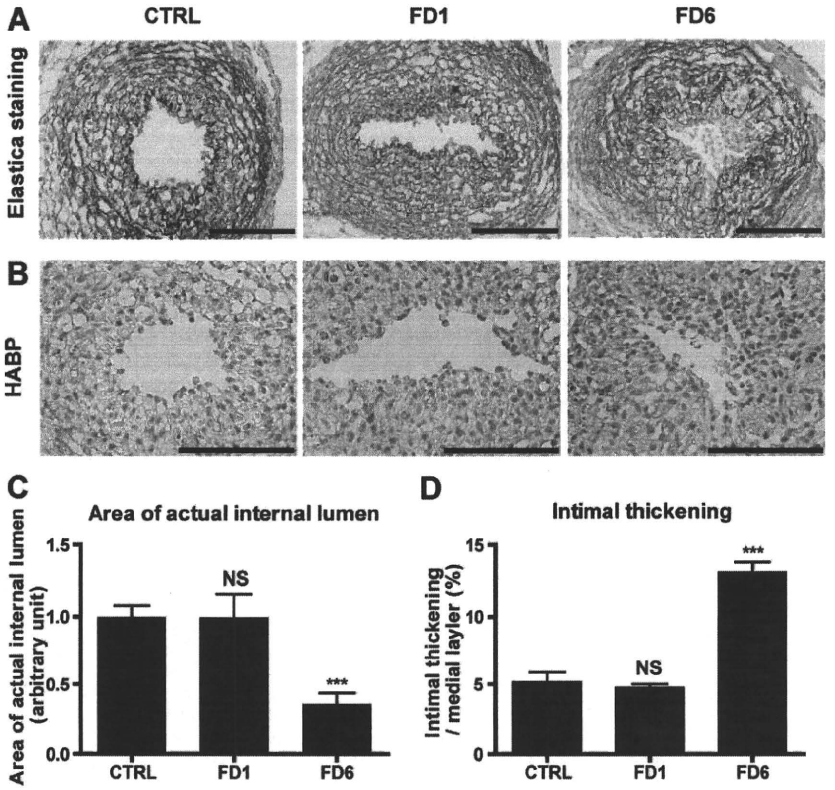

Figure 7. IT in rat DA explants is promoted by FD6. A, Elastica van Gieson staining for DA explants treated with FD1 or FD6. **B,** Strong immunoreaction to hyaluronan in DA explants cultured with FD6. **C,** The area of the internal lumen of the DA treated with FD6 was significantly decreased (n=6 to 7). **D,** The increased IT in the DA treated with FD6 (n=6 to 7). ***$P<0.001$ vs control (CTRL). **Bars:** 100 μm. HABP indicates hyaluronan-binding protein.

Clinical Implications of Using AC Isoform-Selective Modulations

The manipulation of the contractile state of the DA is important for patients with patent DA and complicated congenital heart diseases. All currently available pharmacological therapies rely on synthetic PGE_1 to dilate the DA and prostaglandin H synthase inhibitors to close it. Because these therapies basically change the plasma and/or local concentra-

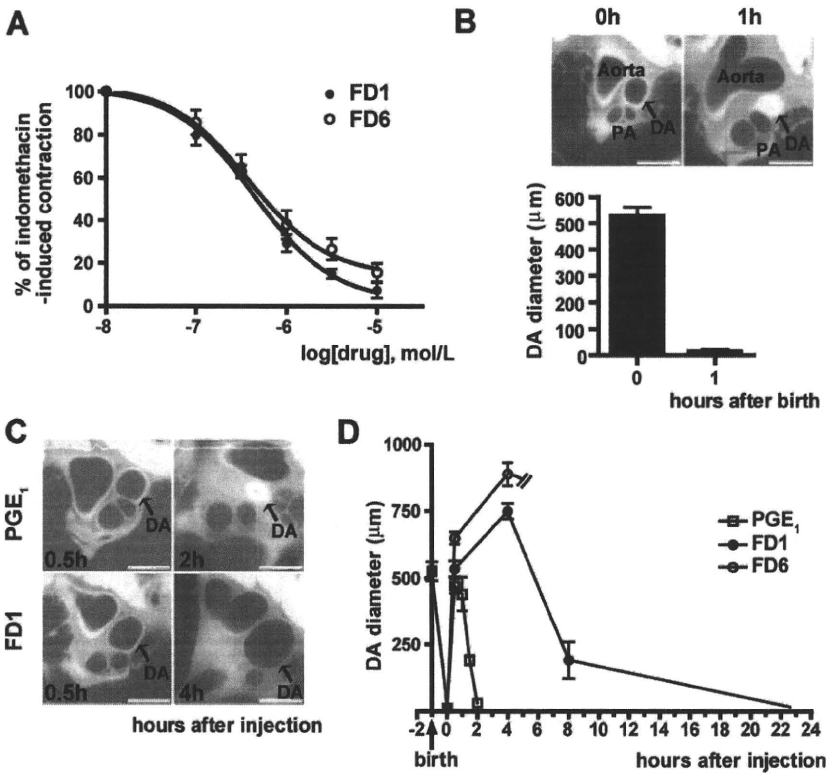

Figure 8. The effects of FD1 and FD6 on vasodilation. A, FD1 and FD6 similarly attenuated indomethacin-induced contraction in DA explants in a dose-dependent manner (n=4 to 10). **B,** The whole-body freezing method revealed that the rat DA opened widely after birth and closed 1 hour after birth **(arrow)** (n=5). **C,** Representative images of rat DAs treated with PGE_1 and FD1 using the whole-body freezing method. **D,** The vasodilating effects of PGE_1, FD1, or FD6 were compared (n=5 to 7). FD1 had a longer action of duration than did PGE_1. All rats injected with FD6 died 4 hours after injection because of apnea. **Bars:** 1 mm. PA indicates pulmonary artery.

tion of PGE, they broadly affect the contractile state and the cellular responses in other types of smooth muscle and tissues, resulting in severe adverse effects on systemic organs. Moreover, PGE_1 has a short duration of action and induces hyaluronan-mediated IT in the DA. In cases of DA-dependent congenital heart diseases, opening of the DA without induction of IT is of particular necessity until the hemodynamics can be improved through surgery. Although differential regulation of vasodilation and IT is preferable for treatment of patients with DA-dependent congenital cardiac malformations, such a treatment is not currently available. Therefore, selective manipulation should be a desirable direction for novel therapeutic strategies. In the present study, we demonstrated that AC isoform-selective activators differentially regulated vascular tone and remodeling in the DA. Our data imply that AC2/6-selective manipulation could be a novel means of achieving DA vasodilation with only minimal effects on the pulmonary arteries and aorta. Moreover, the AC2/6 activator, FD1 has longer pharmacological effects than does PGE_1. Recent studies from other authors have indicated that specific agonists/antagonists for EP4 specifically regulate ductal prostaglandin signals,[29] which could potentially yield a DA-selective vasodilator or vasoconstrictor. However, it should be noted that the EP4 receptor underwent short-term agonist-induced desensitization,[30] which is a common biological phenomenon involving reduction of responsiveness despite continuous agonist induction. Direct activation of AC may overcome the disadvantages of agonist-induced desensitization and FD1 may be beneficial for patients with DA-dependent congenital heart diseases.

In conclusion, we have shown that AC2 and AC6 exert distinct regulation of vascular tone and play an important role in DA remodeling. AC isoform-selective pharmacotherapy using FD1 may serve as a novel therapeutic strategy for patients with DA-dependent congenital heart diseases and as an alternative to currently available PGE therapy.

Acknowledgments

We thank Dr Kazuo Momma and Drs Hideki Taniguchi, Yun-Wen Zheng, and Atsushi Tanaka for assistance with a whole-body freezing method and fluorescence-activated cell sorting analysis, respectively. We thank Dr Koji Otsu for isolation of caveolae fraction.

Sources of Funding

This work was supported by NIH grants 5P01HL066941, HL081741, and HL088426 (to H.K.H.); the Ministry of Health Labor and Welfare of Japan (to Y.I.); the Ministry of Education, Culture, Sports, Science and Technology of Japan (to Y.I. and S.M.); the Yokohama Foundation for Advanced Medical Science (to U.Y., S.M.); the High-Tech Research Center Project for Private Universities: MEXT (to S.M.); Waseda University Grant for Special Research Projects (to S.M.); the Vehicle Racing Commemorative Foundation (to S.M.); Miyata Cardiology Research Promotion Funds (to U.Y. and S.M.); Takeda Science Foundation (to Y.I., U.Y., and S.M.); the Japan Heart Foundation Research Grant (to U.Y.); the Kowa Life Science Foundation (to U.Y.); the Sumitomo Foundation (to U.Y.); the Cosmetology Research Foundation (to Y.I.); Japan Cardiovascular Research Foundation (to S.M.); the Uehara Memorial Foundation (to U.Y.); the Kitsuen Research Foundation (to Y.I.); the Japan Space Forum (to Y.I.); American Heart Association Grant SDG 0835596D (to K.I.); the American Heart Association Western Affiliate (to T.T.); the Department of Veterans Affairs (to H.K.H.); and the Foundation of University of Medicine & Dentistry of New Jersey High-Impact Collaboration Grant (to K.I.).

Disclosures

None.

References

1. Smith GC. The pharmacology of the ductus arteriosus. *Pharmacol Rev*. 1998;50:35–58.
2. Waleh N, Kajino H, Marrache AM, Ginzinger D, Roman C, Seidner SR, Moss TJ, Fouron JC, Vazquez-Tello A, Chemtob S, Clyman RI. Prostaglandin E2–mediated relaxation of the ductus arteriosus: effects of gestational age on g protein-coupled receptor expression, signaling, and vasomotor control. *Circulation*. 2004;110:2326–2332.
3. Yokoyama U, Minamisawa S, Quan H, Ghatak S, Akaike T, Segi-Nishida E, Iwasaki S, Iwamoto M, Misra S, Tamura K, Hori H, Yokota S, Toole BP, Sugimoto Y, Ishikawa Y. Chronic activation of the prostaglandin receptor EP4 promotes hyaluronan-mediated neointimal formation in the ductus arteriosus. *J Clin Invest*. 2006;116:3026–3034.
4. Sunahara RK, Taussig R. Isoforms of mammalian adenylyl cyclase: multiplicities of signaling. *Mol Interv*. 2002;2:168–184.
5. Tang WJ, Gilman AG. Adenylyl cyclases. *Cell*. 1992;70:869–872.
6. Ishikawa Y. Isoform-targeted regulation of cardiac adenylyl cyclase. *J Cardiovasc Pharmacol*. 2003;41(Suppl 1):S1–S4.
7. Bulin C, Albrecht U, Bode JG, Weber AA, Schror K, Levkau B, Fischer JW. Differential effects of vasodilatory prostaglandins on focal adhesions, cytoskeletal architecture, and migration in human aortic smooth muscle cells. *Arterioscler Thromb Vasc Biol*. 2005;25:84–89.
8. Fujino T, Yuhki K, Yamada T, Hara A, Takahata O, Okada Y, Xiao CY, Ma H, Karibe H, Iwashima Y, Fukuzawa J, Hasebe N, Kikuchi K, Narumiya S, Ushikubi F. Effects of the prostanoids on the proliferation or hypertrophy of cultured murine aortic smooth muscle cells. *Br J Pharmacol*. 2002;136:530–539.
9. Indolfi C, Avvedimento EV, Di Lorenzo E, Esposito G, Rapacciuolo A, Giuliano P, Grieco D, Cavuto L, Stingone AM, Ciullo I, Condorelli G, Chiariello M. Activation of cAMP-PKA signaling in vivo inhibits smooth muscle cell proliferation induced by vascular injury. *Nat Med*. 1997;3:775–779.
10. Wang CY, Aronson I, Takuma S, Homma S, Naka Y, Alshafie T, Brovkovych V, Malinski T, Oz MC, Pinsky DJ. cAMP pulse during preservation inhibits the late development of cardiac isograft and allograft vasculopathy. *Circ Res*. 2000;86:982–988.
11. Slomp J, van Munsteren JC, Poelmann RE, de Reeder EG, Bogers AJ, Gittenberger-de Groot AC. Formation of intimal cushions in the ductus arteriosus as a model for vascular intimal thickening. An immunohistochemical study of changes in extracellular matrix components. *Atherosclerosis*. 1992;93:25–39.
12. Pasricha PJ, Hassoun PM, Teufel E, Landman MJ, Fanburg BL. Prostaglandins E1 and E2 stimulate the proliferation of pulmonary artery smooth muscle cells. *Prostaglandins*. 1992;43:5–19.
13. Yau L, Zahradka P. PGE(2) stimulates vascular smooth muscle cell proliferation via the EP2 receptor. *Mol Cell Endocrinol*. 2003;203:77–90.
14. Onda T, Hashimoto Y, Nagai M, Kuramochi H, Saito S, Yamazaki H, Toya Y, Sakai I, Homcy CJ, Nishikawa K, Ishikawa Y. Type-specific regulation of adenylyl cyclase. Selective pharmacological stimulation and inhibition of adenylyl cyclase isoforms. *J Biol Chem*. 2001;276:47785–47793.
15. Iwatsubo K, Minamisawa S, Tsunematsu T, Nakagome M, Toya Y, Tomlinson JE, Umemura S, Scarborough RM, Levy DE, Ishikawa Y. Direct inhibition of type 5 adenylyl cyclase prevents myocardial apoptosis without functional deterioration. *J Biol Chem*. 2004;279:40938–40945.
16. Sutkowski EM, Robbins JD, Tang WJ, Seamon KB. Irreversible inhibition of forskolin interactions with type I adenylyl cyclase by a 6-isothiocyanate derivative of forskolin. *Mol Pharmacol*. 1996;50:299–305.
17. Okumura S, Takagi G, Kawabe J, Yang G, Lee MC, Hong C, Liu J, Vatner DE, Sadoshima J, Vatner SF, Ishikawa Y. Disruption of type 5 adenylyl cyclase gene preserves cardiac function against pressure overload. *Proc Natl Acad Sci U S A*. 2003;100:9986–9990.

18. Tang T, Gao MH, Lai NC, Firth AL, Takahashi T, Guo T, Yuan JX, Roth DM, Hammond HK. Adenylyl cyclase type 6 deletion decreases left ventricular function via impaired calcium handling. *Circulation*. 2008; 117:61–69.
19. Yokoyama U, Minamisawa S, Adachi-Akahane S, Akaike T, Naguro I, Funakoshi K, Iwamoto M, Nakagome M, Uemura N, Hori H, Yokota S, Ishikawa Y. Multiple transcripts of Ca2+ channel alpha1-subunits and a novel spliced variant of the alpha1C-subunit in rat ductus arteriosus. *Am J Physiol Heart Circ Physiol*. 2006;290:H1660–H1670.
20. Gao M, Ping P, Post S, Insel PA, Tang R, Hammond HK. Increased expression of adenylylcyclase type VI proportionately increases beta-adrenergic receptor-stimulated production of cAMP in neonatal rat cardiac myocytes. *Proc Natl Acad Sci U S A*. 1998;95:1038–1043.
21. Wang Y, Huang S, Sah VP, Ross J Jr, Brown JH, Han J, Chien KR. Cardiac muscle cell hypertrophy and apoptosis induced by distinct members of the p38 mitogen-activated protein kinase family. *J Biol Chem*. 1998;273:2161–2168.
22. Yokoyama U, Minamisawa S, Quan H, Akaike T, Suzuki S, Jin M, Jiao Q, Watanabe M, Otsu K, Iwasaki S, Nishimaki S, Sato M, Ishikawa Y. Prostaglandin E2-activated Epac promotes neointimal formation of the rat ductus arteriosus by a process distinct from that of cAMP-dependent protein kinase A. *J Biol Chem*. 2008;283:28702–28709.
23. Akaike T, Jin MH, Yokoyama U, Izumi-Nakaseko H, Jiao Q, Iwasaki S, Iwamoto M, Nishimaki S, Sato M, Yokota S, Kamiya Y, Adachi-Akahane S, Ishikawa Y, Minamisawa S. T-type Ca2+ channels promote oxygenation-induced closure of the rat ductus arteriosus not only by vasoconstriction but also by neointima formation. *J Biol Chem*. 2009;284: 24025–24034.
24. Momma K, Toyoshima K, Takeuchi D, Imamura S, Nakanishi T. In vivo reopening of the neonatal ductus arteriosus by a prostanoid EP4-receptor agonist in the rat. *Prostaglandins Other Lipid Mediat*. 2005;78:117–128.
25. Yokoyama U, Patel HH, Lai NC, Aroonsakool N, Roth DM, Insel PA. The cyclic AMP effector Epac integrates pro- and anti-fibrotic signals. *Proc Natl Acad Sci U S A*. 2008;105:6386–6391.
26. Rabinovitch M, Beharry S, Bothwell T, Jackowski G. Qualitative and quantitative differences in protein synthesis comparing fetal lamb ductus arteriosus endothelium and smooth muscle with cells from adjacent vascular sites. *Dev Biol*. 1988;130:250–258.
27. Wong ST, Baker LP, Trinh K, Hetman M, Suzuki LA, Storm DR, Bornfeldt KE. Adenylyl cyclase 3 mediates prostaglandin E_2-induced growth inhibition in arterial smooth muscle cells. *J Biol Chem*. 2001;276:34206–34212.
28. Gros R, Ding Q, Chorazyczewski J, Pickering JG, Limbird LE, Feldman RD. Adenylyl cyclase isoform-selective regulation of vascular smooth muscle proliferation and cytoskeletal reorganization. *Circ Res*. 2006;99: 845–852.
29. Kajino H, Taniguchi T, Fujieda K, Ushikubi F, Muramatsu I. An EP4 receptor agonist prevents indomethacin-induced closure of rat ductus arteriosus in vivo. *Pediatr Res*. 2004;56:586–590.
30. Nishigaki N, Negishi M, Ichikawa A. Two Gs-coupled prostaglandin E receptor subtypes, EP2 and EP4, differ in desensitization and sensitivity to the metabolic inactivation of the agonist. *Mol Pharmacol*. 1996; 50:1031–1037.

Novelty and Significance

What Is Known?

- Prostaglandin (PG)E-adenylyl cyclase (AC)-cAMP signaling opens the ductus arteriosus (DA) by vasodilation and closes it by hyaluronan-mediated intimal thickening.
- Differential regulation of vasodilation and remodeling of the DA is required for patients with DA-dependent congenital heart diseases after birth.

What New Information Does This Article Contribute?

- AC type 6 (AC6) is involved in vasodilation and hyaluronan-mediated intimal thickening.
- AC type 2 (AC2) inhibits AC6-induced intimal thickening.
- Stimulation of both AC2 and AC6 by the new forskolin derivative FD1 induced long-lasting vasodilation without intimal thickening in the DA.

PGE plays 2 opposing roles in the DA: it induces opening of the DA by vasodilation, and closure by hyaluronan-mediated intimal thickening. Dilation of the DA, but not intimal thickening, is necessary in patients with DA-dependent congenital heart diseases after birth. However, the currently available PGE therapy is not able to differentially regulate vasodilation and intimal thickening in the DA. Our results suggest that AC6 plays a primary role in hyaluronan-mediated vascular remodeling and vasodilation in the DA and that AC2 has an inhibitory effect on AC6-mediated vascular remodeling. We found that stimulation of both AC2 and AC6 by the forskolin derivative FD1 induced long-lasting vasodilation without intimal thickening in the DA. For the first time, we demonstrated that AC2 and AC6 exert distinct regulation of vascular tone and remodeling. In particular, our identification of the interaction of two signaling pathways of AC isoforms in vascular remodeling is novel. AC isoform-selective pharmacotherapy using FD1 may yield a new therapeutic strategy for patients with DA-dependent congenital heart diseases who require DA opening, but not DA closure, through hyaluronan-mediated neointimal thickening. This may become an alternative to the currently available PGE therapy.

THE JOURNAL OF BIOLOGICAL CHEMISTRY VOL. 285, NO. 31, pp. 24248–24259, July 30, 2010

Differential Roles of Epac in Regulating Cell Death in Neuronal and Myocardial Cells*[S]

Received for publication, December 21, 2009, and in revised form, May 13, 2010 Published, JBC Papers in Press, June 1, 2010, DOI 10.1074/jbc.M109.094581

Sayaka Suzuki[‡], Utako Yokoyama[‡1], Takaya Abe[§], Hiroshi Kiyonari[§], Naoya Yamashita[¶], Yuko Kato[‡], Reiko Kurotani[‡], Motohiko Sato[‡], Satoshi Okumura[‡], and Yoshihiro Ishikawa[‡‖]

From the [‡]Cardiovascular Research Institute and [¶]Department of Molecular Pharmacology and Neurobiology, Yokohama City University Graduate School of Medicine, Yokohama 236-0004, Japan, the [§]Laboratory for Animal Resources and Genetic Engineering, RIKEN Center for Developmental Biology, Kobe 650-0047, Japan, and the [‖]Cardiovascular Research Institute, Departments of Cell Biology and Molecular Medicine, and the Department of Medicine, New Jersey Medical School-University of Medicine and Dentistry of New Jersey, Newark, New Jersey 07103

Cell survival and death play critical roles in tissues composed of post-mitotic cells. Cyclic AMP (cAMP) has been known to exert a distinct effect on cell susceptibility to apoptosis, protecting neuronal cells and deteriorating myocardial cells. These effects are primarily studied using protein kinase A activation. In this study we show the differential roles of Epac, an exchange protein activated by cAMP and a new effector molecule of cAMP signaling, in regulating apoptosis in these cell types. Both stimulation of Epac by 8-*p*-methoxyphenylthon-2′-*O*-methyl-cAMP and overexpression of Epac significantly increased DNA fragmentation and TUNEL (terminal deoxynucleotidyltransferase-mediated biotin nick end-labeling)-positive cell counts in mouse cortical neurons but not in cardiac myocytes. In contrast, stimulation of protein kinase A increased apoptosis in cardiac myocytes but not in neuronal cells. In cortical neurons the expression of the Bcl-2 interacting member protein (Bim) was increased by stimulation of Epac at the transcriptional level and was decreased in mice with genetic disruption of Epac1. Epac-induced neuronal apoptosis was attenuated by the silencing of Bim. Furthermore, Epac1 disruption *in vivo* abolished the 3-nitropropionic acid-induced neuronal apoptosis that occurs in wild-type mice. These results suggest that Epac induces neuron-specific apoptosis through increasing Bim expression. Because the disruption of Epac exerted a protective effect on neuronal apoptosis *in vivo*, the inhibition of Epac may be a consideration in designing a therapeutic strategy for the treatment of neurodegenerative diseases.

Induction of apoptosis in post-mitotic cells, such as neurons and cardiac myocytes, has been thought to be responsible for such irreversible disorders as Alzheimer and Huntington diseases as well as stroke and heart failure (1). The effect on cell death of cyclic AMP (cAMP), a major second messenger, has been extensively studied. In neuronal cells it is well known that activation of cAMP signals reduces the rate of neuronal cell death under a variety of stresses (*i.e.* β-amyloid protein, sialoglycopeptide, low potassium-induced neurotoxicity) (2–4), although there have been several reports that dopamine or prostanoid receptor-mediated cAMP production induces neurotoxicity (5, 6). β-Adrenergic receptor signaling, on the other hand, promotes apoptosis in cardiac myocytes, resulting in heart failure (7, 8). Therefore, the model proposing that cAMP signaling plays a protective role in neuronal cells but a deteriorative role in myocardial cells is well accepted.

Most studies that have demonstrated the effect of cAMP signaling on apoptosis have focused primarily on protein kinase A (PKA),[2] a classic target molecule of cAMP. Recent studies involving cAMP signaling have focused instead on Epac, an exchange protein activated by cAMP that has been identified as a new target of cAMP, independent of PKA (9). Epac has been found to regulate a variety of cellular processes, including cell proliferation, migration, secretion, and differentiation (10). It has been demonstrated that Epac either alone or with PKA plays a protective role in immune cells against apoptosis (11, 12). In post-mitotic cells such as neurons and cardiac myocytes, however, the role of Epac in apoptosis has not been reported.

To date two isoforms of Epac have been identified, Epac1 and Epac2 (9); they differ in that Epac2 contains a second binding site for cAMP. It has recently been reported that there is an up-regulation of Epac1 mRNA in Alzheimer disease (13) and an up-regulation of Epac1 protein expression in rats with inflamed neurons (14), implicating that cAMP signaling may not always play a protective role in neurons. The change in the Epac1 expression pattern has also been demonstrated in other cell

* This work was supported by a grant-in-aid for Scientific Research (KAKENHI) (to U. Y. and S. S.) and by grants from the Ministry of Health, Labor, and Welfare (to Y. I.), the Ministry of Education, Culture, Sports, Science, and Technology of Japan (to Y. I.), the Yokohama Foundation for Advanced Medical Science (to U. Y.), the Kanae Foundation for the Promotion for Medical Science (to U. Y.), the Miyata Cardiology Research Promotion Funds (to U. Y.), the Takeda Science Foundation (to U. Y.), the Sumitomo Foundation (to U. Y.), the Japan Heart Foundation Research Grant (to U. Y.), the Kowa Life Science Foundation (to U. Y.), the Cosmetology Research Foundation (to Y. I.), the Uehara Memorial Foundation (to U. Y.), the Kitsuen Research Foundation (to Y. I.), and the Japan Space Forum (to Y. I.).

[S] The on-line version of this article (available at http://www.jbc.org) contains supplemental Methods and Figs. 1–7.

[1] To whom correspondence should be addressed: Cardiovascular Research Institute, Yokohama City University Graduate School of Medicine, 3-9 Fukuura, Kanazawa-ku, Yokohama 236-0004, Japan. Tel.: 81-45-787-2575; Fax: 81-45-788-1470; E-mail: utako@yokohama-cu.ac.jp.

[2] The abbreviations used are: PKA, protein kinase A; Bim, Bcl-2 interacting member protein; pMe-cAMP, 8-*p*-methoxyphenylthon-2′-*O*-methyl-cAMP; Bnz-cAMP, N^6-benzoyladenosine-cAMP; RT, reverse transcription; TUNEL, terminal deoxynucleotidyltransferase-mediated biotin nick end-labeling; 3-NP, 3-propionic acid; siRNA, small interfering RNA; DAPI, 4′,6-diamidino-2-phenylindole; JNK, c-Jun N-terminal kinase; MAPK, mitogen-activated protein kinase; KO, knock-out.

types (*i.e.* heart, vasculature, kidney, and lung) (15–18). The stoichiometry of Epac, especially of Epac1, and that of PKA might be changed in several diseases, including neuronal and cardiac disorders; this could lead to the various effects of cAMP signaling on cell death.

Through experiments using Epac- or PKA-selective cAMP analogs and overexpression of Epac1 and the PKA catalytic subunit and Epac1-deficient mice, the present study demonstrates that cAMP signaling no longer increases neuronal cell viability when Epac is selectively activated: instead, cAMP signaling induces apoptosis through increasing Bcl-2 interacting member protein (Bim) expression. Our findings also suggest that the selective inhibition of Epac signaling may become a therapeutic strategy in the treatment of neurodegenerative diseases.

EXPERIMENTAL PROCEDURES

Antibodies and Reagents—8-*p*-Methoxyphenylthon-2′-*O*-methyl-cAMP (pMe-cAMP) and N^6-benzoyladenosine-cAMP (Bnz-cAMP) were purchased from BioLog Life Science Institute (Bremen, Germany) and Sigma, respectively. Antibodies to Epac1, Epac2, and a PKA α catalytic subunit were obtained from Santa Cruz Biotechnology (Santa Cruz, CA). An antibody to Bim was purchased from Stressgen Biotechnologies (Victoria, BC, Canada). Antibodies to Bim and cleaved caspase 3 were purchased from Cell Signaling Technology (Danvers, MA). An antibody to Bcl-2 was purchased from BD Biosciences.

Generation of Epac1 Knock-out Mice—Epac1 knock-out mice (Epac1 KO; accession number CDB0542K (LARGE (Laboratory for Animal Resources and Genetic Engineering)) were generated by means of homologous recombination (19). Briefly, the targeting vector was constructed by inserting loxP/PGK-Neo-pA/loxP (LARGE) into exon 1 and exon 2 of the genomic Epac1 locus (see Fig. 7*A*). The targeting vector was introduced into TT2 embryonic stem cells, and homologous recombinant clones were first identified by PCR, then confirmed by Southern blot analysis (see Fig. 7*B*). The targeted embryonic stem cell clones were injected into CD-1 8-cell stage embryos, and the resultant male chimeras were mated with C57BL/6 females to establish germ line transmission. All experiments were performed on C57BL/6 and CBA mixed-background 3–5-month-old male homozygous Epac1 KO and wild type (WT) littermates from F1 heterozygote crosses. Mice were genotyped by PCR using a mixture of three primers (F1, TGA GAA GAG CCC CAT CGT TGT G; B1, GCC TGG CAC ATG GAA GTG AT; NeoF1, TGA ATG GAA GGA TTG GAG CTA CG) as indicated in Fig. 7*A*. The PCR conditions consisted of 95 °C for 5 min, 35 cycles of 95 °C for 30 s each, 60 °C for 30 s, and 72 °C for 30 s followed by 72 °C for 7 min (Fig. 7*C*).

All experiments were performed on 3–5-month-old homozygous Epac1 KO mice and WT littermates. This study was approved by the Animal Care and Use Committee at Yokohama City University School of Medicine.

Primary Culture of Fetal Mouse Cortical Neurons—Primary cortical neurons were isolated from the cortices of embryonic day 15–17 C57BL/6 or Epac1 KO mice, as previously described (20) with some modifications. Briefly, the cortex was incubated with 0.3% trypsin (Invitrogen) by titration; then cells were plated onto a 12-mm glass coverslip precoated with 6 mg/ml poly-L-lysine (Wako Pure Chemical Industries, Osaka, Japan) at a density of 1×10^5 cells/glass. The cells were incubated at 37 °C with 5% CO_2, 95% atmospheric air in a neurobasal medium containing 1× GlutaMAX-1, B-27 supplement (Invitrogen), 100 μg/ml penicillin, and 100 μg/ml streptomycin. Cells were used in experiments 4–7 days later.

Primary Culture of Neonatal Mouse Cardiac Myocytes—Cardiac myocytes were isolated from the hearts of 1-day-old mice as previously described (21) with some modifications. Briefly, myocytes were chopped into small pieces and digested with 0.1% collagenase type II and 0.04% pancreatin 3 times at 7-min intervals. To remove the non-myocyte fraction, the cells were plated onto culture dishes in minimum essential medium (Invitrogen) with 10% fetal bovine serum containing 100 μg/ml penicillin and 100 μg/ml streptomycin for 45 min, after which the non-attached myocyte-rich fraction was plated onto a 12-mm glass coverslip precoated with 20 mg/ml laminin (Sigma) at a density of 1×10^5 cells/glass in the same medium. Twenty-four hours after plating, the culture medium was changed to minimum essential medium with an insulin-transferrin-selenium-A supplement (ITS-A, Invitrogen) containing 100 μg/ml penicillin and 100 μg/ml streptomycin. The cells were maintained in a humidified 5% CO_2, 95% atmospheric air incubator at 37 °C.

Primary Culture of Mouse Renal Epithelial Cells—Primary culture of mouse renal epithelial cells was performed as previously described (22).

Quantitative Reverse Transcription (RT)-PCR—Total RNA was extracted from cortical neurons using TRIzol (Invitrogen) according to the manufacturer's instructions. Both the generation of cDNA and the RT-PCR analysis were performed as previously described (17, 23). Real-time PCR was executed using a MyiQ Single-Color Real-Time PCR Detection System (Bio-Rad) and an SYBR Green kit (Takara Bio, Shiga, Japan). Primers for amplification were designed based on Bim (5′-CCCGGAGATACGGATTGCAC-3′ and 5′- GCCTCGCGGTAATCATTTGC-3′) and 18 S ribosomal RNA. The forward and reverse primer set was designed between multiple exons. Abundance of mRNA was determined relative to that of 18 S ribosomal RNA.

Northern Blotting—Partial fragments of mouse Epac1 and Epac2 cDNA clones were obtained by PCR. A mouse glyceraldehyde-3-phosphate dehydrogenase probe was used as an internal control. Northern blotting was performed as previously described (24).

Western Blot Analysis—Western blot analysis of cortical neurons and cardiac myocytes was performed as previously described (25) with some modifications. Briefly, cells in 35-mm plastic dishes were lysed and collected with a lysis buffer (25 mM Tris-HCl (pH 8.0), 10 mM EGTA, 10 mM EDTA, 10 mM $Na_4P_2O_7$, 100 mM NaF, 10 mM Na_3VO_4, 20 μg/ml 1-chloro-3-tosylamido-7-amino-2-heptanone or N^{α}-*p*-tosyl-L-lysine chloromethyl ketone, 10 μg/ml leupeptin, 1 mM phenylmethylsulfonyl fluoride, 50 units of erythrina trypsin inhibitor, 2 μg/ml aprotinin, and 1% Nonidet P-40). After protein concentrations were determined using the RC DC protein assay kit (Bio-Rad), SDS-PAGE and Western blotting were performed followed by densitometric analysis using LAS3000 and Science Lab Multi Gauge Version 3.0 software (Fujifilm, Tokyo, Japan).